

TROPICAL SECANT GRAPHS OF MONOMIAL CURVES

MARÍA ANGÉLICA CUETO AND SHAOWEI LIN

ABSTRACT. The first secant variety of a projective monomial curve is a threefold with an action by a one-dimensional torus. Its tropicalization is a three-dimensional fan with a one-dimensional lineality space, so the tropical threefold is represented by a balanced graph. Our main result is an explicit construction of that graph. As a consequence, we obtain algorithms to effectively compute the multidegree and Chow polytope of an arbitrary projective monomial curve. This generalizes an earlier degree formula due to Ranestad. The combinatorics underlying our construction is rather delicate, and it is based on a refinement of the theory of geometric tropicalization due to Hacking, Keel and Tevelev.

1. INTRODUCTION

In this paper, we define and study four graphs that hide rich geometry: an abstract graph (the *abstract tropical secant surface graph*), a weighted graph in \mathbb{R}^{n+1} (the *tropical secant surface graph* or *master graph*), a weighted graph in the $(n-2)$ -sphere (the *tropical secant graph*) and, finally, a weighted graph representing a simplicial spherical complex (the *Gröbner tropical secant graph*). All four graphs are parameterized by a sequence of n coprime distinct positive integers i_1, \dots, i_n , where $n \geq 4$. As their names suggest, these graphs are stepping stones to constructing either a tropical surface or the tropicalization of a secant variety.

In recent years, tropical geometry has provided a new approach to attack implicitization problems [7, 10, 19, 20]. We tropicalize classical varieties to obtain weighted polyhedral fans with the hope of recovering useful algebro-geometric information by working on the polyhedral-geometric side. Our paper illustrates this principle with a family of classical secant threefolds: the first secant variety of a monomial projective curve $(1 : t^{i_1} : \dots : t^{i_n})$. By definition, the secant variety of the curve is the closure of the union of all lines that meet the curve in two distinct points. These varieties have been studied extensively in the literature; see [5, 18] and references therein for more details. One of the main contributions of this paper is a complete characterization of their tropical counterparts, which is carried out in full detail in Section 5. More precisely,

Theorem 1.1. *Given a monomial curve C in \mathbb{P}^n parameterized by n distinct coprime positive integers $\{i_1, \dots, i_n\}$, the tropicalization of its first secant variety is the cone from the vector space $\mathbb{R}\langle \mathbf{1}, (0, i_1, \dots, i_n) \rangle$ over the tropical secant graph of the curve.*

Strictly contained in this tropical variety is the first tropical secant complex of the monomial curve (Propositions 7.2 and 7.4). This complex has recently been investigated by Develin and Draisma in [9, 11] in an attempt to study secant varieties of toric varieties via tropicalizations.

2010 *Mathematics Subject Classification.* 14Q05, 14T05 (Primary); 14M25 (Secondary).

Key words and phrases. Monomial curves, secant varieties, resolution graphs, tropical implicitization, Newton polytope.

M.A. Cueto was supported by a UC Berkeley Chancellor's Fellowship and S. Lin was supported by a Singapore A*STAR Fellowship.

Unfortunately, computing the tropicalization of an algebraic variety without any information about its defining ideal is not an easy task. This new point of view was pioneered by the work of Kapranov and his collaborators [13], and further developed by Hacking, Keel and Tevelev [15], and by the first author [6]. This new theory, known as *geometric tropicalization* (Theorem 4.1), relies on a parametric representation of the variety and the characterization of tropicalizations of algebraic varieties in terms of *divisorial valuations*, following the spirit of [1]. To do so, we need to provide a normal \mathbb{Q} -factorial compactification of the given variety, satisfying suitable boundary properties. This can be quite difficult to perform if the variety is non-generic. We can see this from the extensive number of pages we devote to computing the master graph using this technique, and also from the small sample of numerical examples available in the literature.

As we explain in Section 4, the main obstacle to apply this theory for non-generic surfaces lies in finding a suitable (tropical) compactification of the given variety whose boundary has simple normal crossings, a condition which can be further relaxed to *combinatorial normal crossings* [6, 19]. In the surface case, This last condition requires a divisorial boundary where no three boundary components meet at a point. In principal, this can be achieved by modifying any given compactification by blow-ups of isolated surface singularities, and the difficulty becomes algebraic, since we need to carry all valuations along the different blow-ups.

In practice, knowing which points to blow up and how to carry the geometric information on the boundary along the various blow-ups performed can be a combinatorial challenge. However, the surfaces studied in this paper have a very rich combinatorial structure, and we can make full use of this feature to compute their tropicalizations using resolutions. Our methods allow us to read off this tropical variety directly from the master graph, which encodes the resolution diagrams of the surface at each singular point (see Figure 1). This is explained in detail in Sections 3 and 4, in particular in Theorem 3.2. This construction provides a compactification of the toric arrangement given by the $n + 1$ binomial curves $(w^{i_j} - \lambda = 0)$ in \mathbb{T}^2 , for $0 \leq j \leq n$. Such compactifications have been studied recently by L. Moci [17]. His construction, closely related to ours in spirit, realizes the wonderful compactification of De Concini and Procesi [8].

In Section 6, we exploit these tropical secant graphs to recover geometric information about the first secant varieties of monomial curves. More precisely, we recover their multidegrees with respect to the rank two lattice generated by the all-one's vector and the exponent vectors of the curves, following algorithms from [7, 10]. The degree of these threefolds was previously worked out by Ranestad in [18] and, unsurprisingly, our methods give similar combinatorial formulas in terms of the exponents i_1, \dots, i_n . The main advantage of our approach is that, with the same effort, we can provide much more information about these varieties, including their *Chow polytopes*.

Our construction is particularly enlightening in the case when $n = 4$, where the threefold secant variety becomes a hypersurface. In this special situation, we recover the Newton polytope of the defining equation. Although the lack of a fan structure in our description of this tropical variety is not an issue in our methods, it would be desirable to have one to predict extra combinatorial information about the Newton polytope, such as the number of facets. For this reason, we devote the last part of Section 6 to refining the presentation of the tropical secant graphs to turn them into weighted simplicial complexes. These structures are inherited from the Gröbner fan structure of the defining ideals and from the coarsest fan structure of the tropical threefolds. We choose the name *Gröbner tropical secant graph* to highlight this property. We illustrate all our constructions and results with the sequence $\{30, 45, 55, 78\}$, inspired by [18, Example 3.3], and with the rational normal curve (Example 7.1).

Although secant varieties have been extensively studied in the past, we hope our work illustrates the power of *tropical implicitization* and how it can be used to go beyond standard implicitization methods even when looking at classical examples.

2. THE MASTER GRAPH

In this section, we describe the main object of this paper: the master graph. We start by defining an abstract graph parameterized by n coprime positive integers i_1, \dots, i_n . Throughout the paper, we set $n \geq 4$. To simplify notation, we call $i_0 = 0$ and we assume $0 < i_1 < i_2 < \dots < i_n$. We build this graph by gluing two types of graphs along common labeled nodes: two caterpillar graphs $G_{E,D}$, $G_{h,D}$ and a family of star graphs $\{G_{F_{\underline{a}},D}\}_{\underline{a}}$ parameterized by suitable subsets \underline{a} of the index set $\{0, i_1, \dots, i_n\}$. We call this abstract graph the *abstract tropical secant surface graph*.

Our first building block is the caterpillar graph $G_{E,D}$, as illustrated on the top-left side of Figure 1. It consists of $2n - 1$ nodes and $2n - 2$ edges. Nodes are grouped in two levels, with labels $E_{i_1}, \dots, E_{i_{n-1}}$ and D_{i_1}, \dots, D_{i_n} . Similarly, our second graph, denoted by $G_{h,D}$ and depicted on the bottom-left side of Figure 1, consists of $2n$ nodes grouped in two levels with labels $h_{i_1}, \dots, h_{i_{n-1}}$ and $D_0, D_{i_1}, \dots, D_{i_n}$ respectively, and $2n - 1$ edges.

The third family of graphs consists of star trees and it is denoted by $\{G_{F_{\underline{a}},D}\}_{\underline{a}}$. These graphs are parameterized by sets of size at least two, obtained by intersecting an arithmetic progression of integer numbers with the index set $\{0, i_1, \dots, i_n\}$. They are illustrated in the rightmost picture in Figure 1. We allow the common difference of these progressions to be 1, so the set of all exponents $\{0, i_1, \dots, i_n\}$ is a valid subset. The size of the subset \underline{a} associated to an arithmetic progression coincides with the degree of the corresponding node $F_{\underline{a}}$ in the abstract graph. Note that several arithmetic progressions can give the same subset of $\{0, i_1, \dots, i_n\}$, and hence the same node $F_{\underline{a}}$ in the graph $G_{F_{\underline{a}},D}$. If $\underline{a} = \{i_{j_1}, \dots, i_{j_k}\}$, then the graph has $k + 1$ nodes and k edges: k nodes labeled $D_{i_{j_1}}, \dots, D_{i_{j_k}}$ and a central node $F_{\underline{a}}$, connected to the other k nodes in the graph. As Example 2.3 reveals, only nodes of degree at least three are relevant for our constructions, so in principle we should only consider subsets of size at least three. However, to simplify our statements, we allow subsets of size two as well.

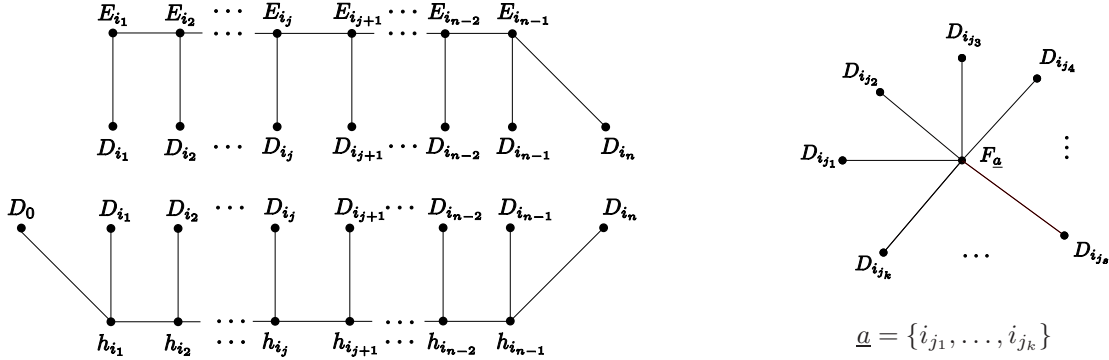


FIGURE 1. The graphs $G_{E,D}$, $G_{h,D}$ and $\{G_{F_{\underline{a}},D}\}_{\underline{a}}$ glue together to form the *master graph*.

We realize the abstract tropical secant surface graph in \mathbb{R}^{n+1} by mapping each node to an integer vector and extending linearly on all edges. Our chosen map has additional data: a weight for each

edge in the graph. We call this weighted graph the *tropical secant surface graph* or *master graph*. We explain this construction in full detail below. For a numerical example, see Figure 2.

Definition 2.1. *The master graph is a weighted graph in \mathbb{R}^{n+1} parameterized by n distinct coprime numbers $\{i_1, \dots, i_n\}$ with nodes:*

- (i) $D_{i_j} = e_j := (0, \dots, 0, 1, 0, \dots, 0) \quad (0 \leq j \leq n)$,
- (ii) $E_{i_j} = (0, i_1, \dots, i_{j-1}, i_j, \dots, i_j) \quad h_{i_j} = (-i_j, \dots, -i_j, -i_{j+1}, \dots, -i_n) \quad (1 \leq j \leq n-1)$,
- (iii) $F_{\underline{a}} = \sum_{i_j \in \underline{a}} e_j$ where $\underline{a} \subseteq \{0, i_1, \dots, i_n\}$ has size at least two and is obtained by intersecting an arithmetic progression of integers with the index set $\{0, i_1, \dots, i_n\}$.

Its edges agree with the edges of the abstract tropical secant surface graph, and have weights:

- (i) $m_{D_{i_0}, h_{i_1}} = 1$, $m_{D_{i_n}, E_{i_{n-1}}} = \gcd(i_1, \dots, i_{n-1})$, $m_{D_{i_n}, h_{i_{n-1}}} = i_n$,
- (ii) $m_{D_{i_j}, E_{i_j}} = \gcd(i_1, \dots, i_j)$, $m_{D_{i_j}, h_{i_j}} = \gcd(i_j, \dots, i_n) \quad (1 \leq j \leq n-1)$,
- (iii) $m_{E_{i_j}, E_{i_{j+1}}} = \gcd(i_1, \dots, i_j)$, $m_{h_{i_j}, h_{i_{j+1}}} = \gcd(i_{j+1}, \dots, i_n) \quad (1 \leq j \leq n-2)$,
- (iv) $m_{F_{\underline{a}}, D_{i_j}} = \sum_r \varphi(r)$, where we sum over the common differences r of all arithmetic progressions containing i_j and giving the same subset \underline{a} . Here, φ denotes Euler's phi function.

Remark 2.2. *As we mentioned earlier, if the subset \underline{a} has two elements, say i_j and i_k , then $F_{\underline{a}}$ is a bivalent node and we may eliminate it from the graph if desired, replacing its two adjacent edges by a single edge. Both edges $F_{i_j, i_k} D_{i_j}$ and $F_{i_j, i_k} D_{i_k}$ have the same multiplicity, so we assign this number as the multiplicity of the new edge $D_{i_j} D_{i_k}$.*

From the definition, it is immediate to check that the node E_{i_1} is always bivalent. However, we always keep it in our graph, since this greatly simplifies our constructions.

We illustrate the previous definition with an example. Note that, in general, the master graph may have nodes $F_{\underline{a}}$ with $0 \notin \underline{a}$. This is determined by the combinatorics of the set $\{i_1, \dots, i_n\}$.

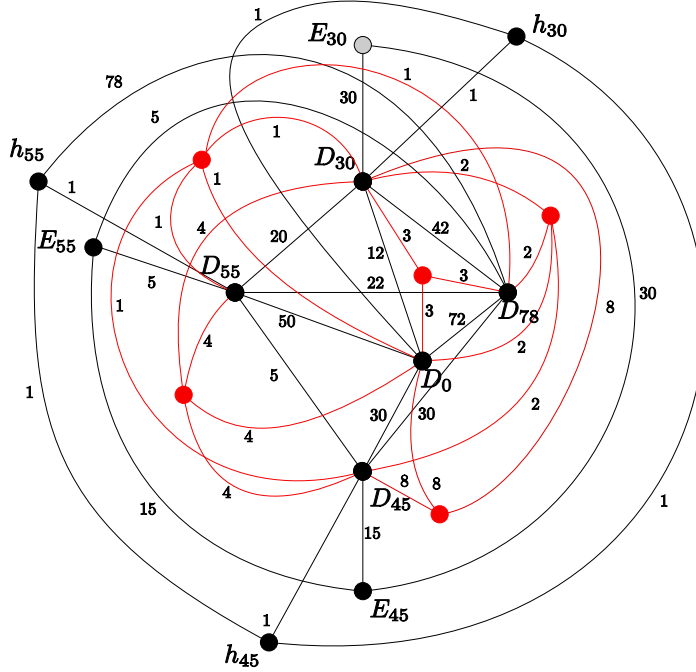
Example 2.3. We compute the master graph associated to the set $\{30, 45, 55, 78\}$. For simplicity, we eliminate all nine bivalent nodes F_{i_j, i_k} from the construction and we keep the bivalent grey node E_{i_1} . The resulting weighted graph has 16 vertices and 36 edges and it is depicted in Figure 2. There are five nodes of type $F_{\underline{a}}$, namely $F_{0,30,45,55,78} = (1, 1, 1, 1, 1)$, $F_{0,30,45,78} = (1, 1, 1, 0, 1)$, $F_{0,30,45,55} = (1, 1, 1, 1, 0)$, $F_{0,30,45} = (1, 1, 1, 0, 0)$ and $F_{0,30,78} = (1, 1, 0, 0, 1)$. They correspond to the five unlabeled nodes in the picture. \diamond

Before stating the main result of this section, we recall the definition of a balanced graph.

Definition 2.4. *Let $(G, m) \subset \mathbb{R}^N$ be a weighted graph where each node has integer coordinates. Let w be a node in G and let $\{w_1, \dots, w_r\}$ be the set of nodes adjacent to w . Consider the primitive lattices $\Lambda_w = \mathbb{R}\langle w \rangle \cap \mathbb{Z}^N$ and $\Lambda_{w, w_i} = \mathbb{R}\langle w, w_i \rangle \cap \mathbb{Z}^N$. Then, $\Lambda_{w, w_i} / \Lambda_w$ is a rank one lattice and it admits a unique generator which lifts to an element in the cone $\mathbb{R}_{\geq 0}\langle w, w_i \rangle \subset \mathbb{R}^N$. Let $u_{w_i|w}$ be one such lifting. We say that the node w is balanced if $\sum_{i=1}^r m_{w_i, w} u_{w_i|w} \in \Lambda_w$. If all nodes of G are balanced, then we say that the weighted graph (G, m) satisfies the balancing condition.*

Theorem 2.5. *The master graph satisfies the balancing condition.*

Proof. We proceed by analyzing the balance at each node, following Definition 2.4. The main difficulty lies in finding the corresponding vector $u_{w_i|w}$ for each edge $w_i w$ in the graph. We define $g_{i_j} := \gcd(i_1, \dots, i_j)$ and $g^{i_j} := \gcd(i_j, \dots, i_n)$. Note that these are the weights $m_{D_{i_j}, E_{i_j}}$ and $m_{D_{i_j}, h_{i_j}}$ of the master graph. To simplify notation, we set $E_{i_0} = E_{i_n} = h_{i_0} = h_{i_n} = \mathbf{0}$, add the edges $E_{i_0} E_{i_1}$, $E_{i_{n-1}} E_{i_n}$, $h_{i_0} h_{i_1}$ and $h_{i_{n-1}} h_{i_n}$ to our graph and assign weight zero to them.

FIGURE 2. The master graph associated to the curve $(1 : t^{30} : t^{45} : t^{55} : t^{78})$.

We start by checking the balance at all nodes E_{i_j} , for $1 \leq j \leq n-1$. In this case, we know that $\Lambda_{E_{i_j}} = \mathbb{Z}\langle E_{i_j}/g_{i_j} \rangle = \mathbb{Z}\langle (0, i_1/g_{i_j}, \dots, i_j/g_{i_j}, \dots, i_j/g_{i_j}) \rangle$ and $\Lambda_{E_{i_j}, D_{i_j}} = \mathbb{Z}\langle E_{i_j}/g_{i_j}, e_j \rangle$. So $u_{D_{i_j}|E_{i_j}} = e_j$. Similarly, we have $u_{D_{i_n}|E_{i_{n-1}}} = e_n$. On the other hand, we know that the lattice $\Lambda_{E_{i_j}, E_{i_{j+1}}}$ equals $\mathbb{R}\langle E_{i_{j+1}}/g_{i_{j+1}}, E_{i_j}/g_{i_j} \rangle \cap \mathbb{Z}^{n+1}$. By definition, we need to extend the primitive vector E_{i_j}/g_{i_j} to a basis of $\Lambda_{E_{i_j}, E_{i_{j+1}}}$ by adding a single vector with appropriate sign. In this case, $u_{E_{i_{j+1}}|E_{i_j}} = \sum_{k=j+1}^n e_k$.

Next, we compute $u_{E_{i_{j-1}}|E_{i_j}}$. Here, $\Lambda = \mathbb{Z}\langle E_{i_{j-1}}/g_{i_{j-1}}, E_{i_j}/g_{i_j} \rangle$ is not a primitive lattice, and we need to extend E_{i_j}/g_{i_j} to a basis of its saturation $\Lambda_{E_{i_{j-1}}, E_{i_j}}$. Our first candidate vector is $(E_{i_j} - E_{i_{j-1}})/(i_j - i_{j-1}) = -\sum_{k=j-1}^n e_k$. However, since $g_{i_{j-1}}$ need not equal g_{i_j} , we need to slightly modify our choice. We set $v = (0, a i_1/g_{i_{j-1}}, \dots, a i_{j-1}/g_{i_{j-1}}, -b, \dots, -b)$, for $a, b \in \mathbb{Z}$ such that $a i_j + b g_{i_{j-1}} = g_{i_j}$. We can check that all nonzero 2×2 -minors of the matrix with rows E_{i_j}/g_{i_j} and v are of the form: $-b i_k/g_{i_j} - (i_j i_k)/(g_{i_j} g_{i_{j-1}}) = -i_k/g_{i_{j-1}}$, for $j-1 \leq k \leq n$. Therefore, their gcd equals one, and E_{i_j}/g_{i_j} and $\pm v$ generate a primitive lattice which contains $E_{i_{j-1}}$ by construction. To determine the correct choice of sign for $\pm v$, we write $E_{i_{j-1}}$ as a linear combination of E_{i_j}/g_{i_j} and v , and we require the coefficient of v to be positive. In this case,

$$E_{i_{j-1}} = g_{i_j}(1 - a(i_j - i_{j-1})/g_{i_j}) \cdot E_{i_j}/g_{i_j} + g_{i_{j-1}}(i_j - i_{j-1})/g_{i_j} \cdot v.$$

Thus, we conclude that $u_{E_{i_{j-1}}|E_{i_j}} = v$ for $j-1 \leq k \leq n$. With these weights, it is straight-forward to check that the graph is balanced at E_{i_j} .

Working with g^{i_j} instead of g_{i_j} , a similar procedure to the one we just described proves that the graph is balanced at the nodes h_{i_j} for all $1 \leq j \leq n-1$. Balance at the nodes $F_{\underline{a}}$ follows by

construction, so it remains to check the balance at the nodes D_{i_j} . In this case, $u_{E_{i_j}|D_{i_j}} = E_{i_j}/g_{i_j}$, $u_{h_{i_j}|D_{i_j}} = h_{i_j}/g^{i_j}$, $u_{F_{\underline{a}}|D_{i_j}} = F_{\underline{a}}$ (for $i_j \in \underline{a}$), and $u_{E_{i_{n-1}}|D_{i_n}} = E_{i_{n-1}}$. The balancing equation is

$$\sum_{\underline{a} \ni i_j} \left(\sum_r \varphi(r) \right) F_{\underline{a}} + E_{i_j} + h_{i_j} = \sum_{k=0}^n \left(\sum_{r \mid |i_k - i_j|} \varphi(r) - |i_k - i_j| \right) e_k.$$

Since $\sum_{l \mid s, l > 0} \varphi(l) = s$, we conclude that the graph is also balanced at D_{i_j} . \square

3. THE MASTER GRAPH IS A TROPICAL SURFACE

In this section, we explain the suggestive name “tropical secant surface graph” for the master graph. More concretely, we show that it is the tropicalization of a surface parameterized by the map $(\lambda, w) \mapsto (1 - \lambda, w^{i_1} - \lambda, \dots, w^{i_n} - \lambda)$. Before that, we review the basics of tropical geometry.

Definition 3.1. *Given an affine variety $X \subset \mathbb{C}^N$ with defining ideal $I = I(X)$, we define the tropicalization of X to be the set*

$$\mathcal{T}X = \mathcal{T}I = \{w \in \mathbb{R}^N : \text{in}_w(I) \text{ does not contain a monomial}\}.$$

Here, $\text{in}_w(I) = \langle \text{in}_w(f) : f \in I \rangle$, and if $f = \sum_{\alpha} c_{\alpha} \underline{x}^{\alpha}$, then $\text{in}_w(f) = \sum_{\alpha \cdot w = W} c_{\alpha} \underline{x}^{\alpha}$, where $W = \min\{\alpha \cdot w : c_{\alpha} \neq 0\}$. If $X \subset \mathbb{P}^N$, then its tropicalization is defined as $\mathcal{T}X' \subset \mathbb{R}^{N+1}$, where X' is the affine cone over X in \mathbb{C}^{N+1} .

Although it may not be clear from Definition 3.1, tropicalizations are toric in nature. More precisely, let $\mathbb{T}^N = (\mathbb{C}^*)^N$ be the algebraic torus. Let Y be a subvariety of \mathbb{T}^N , also known as a *very affine variety*. Suppose $I_Y \subset \mathbb{C}[\mathbb{T}^N] = \mathbb{C}[y_1^{\pm}, \dots, y_N^{\pm}]$ is the defining ideal of Y . We define the tropicalization of $Y \subset \mathbb{T}^N$ as

$$\mathcal{T}Y = \{v \in \mathbb{R}^N : 1 \notin \text{in}_v(I_Y)\}.$$

Here, the initial ideal with respect to a vector v is the same as that in Definition 3.1. Consider the Zariski closure \overline{Y} of Y in \mathbb{C}^N . It is easy to see that $\mathcal{T}Y$ equals $\mathcal{T}\overline{Y}$. Indeed, this follows from the fact that I_Y is the saturation ideal $(I_{\overline{Y}} \mathbb{C}[\mathbb{T}^N] : (y_1 \cdots y_N)^{\infty})$ and $I_{\overline{Y}} = I_Y \cap \mathbb{C}[y_1, \dots, y_N]$. Therefore, if we start with an irreducible variety $X \subset \mathbb{C}^N$ not contained in a coordinate hyperplane, then we can consider the very affine variety $Y = X \cap \mathbb{T}^N$, which has the same dimension as X . The tropical variety $\mathcal{T}Y$ is a pure polyhedral subfan of the Gröbner fan of I and it preserves an important invariant of Y : both objects have the same dimension [1].

Tropical implicitization is a recently developed technique to approach classical implicitization problems [19]. For instance, when Y is a codimension-one hypersurface, $I_Y = \langle g \rangle$ is principal and $\mathcal{T}Y$ is the union of all codimension one cones in the normal fan of the Newton polytope of a polynomial g , so knowing $\mathcal{T}Y$ can help us in finding g . But to achieve this, we need to compute $\mathcal{T}Y$ without explicitly knowing I_Y . We show how to do this in Section 4.

A point $w \in \mathcal{T}X$ is called *regular* if $\mathcal{T}X$ is a linear space locally near w . We can attach a positive integer to each regular point of the tropical variety that carries information about the geometry of X . More precisely, we define the *multiplicity* m_w of a regular point w to be the sum of multiplicities of all minimal associated primes of the initial ideal $\text{in}_w(I)$ [10]. The multiplicity of a maximal cone in $\mathcal{T}X$ agrees with the multiplicity at any of its regular points. One can show that this assignment does not depend on the choice of the regular point and that with these multiplicities, the tropical variety satisfies the *balancing condition* [19, Corollary 3.4].

In the case of projective varieties, or in general, when we have a torus action given by an integer lattice Λ , the tropical variety $\mathcal{T}X$ has a *lineality space*, that is, the maximal linear space contained

in all cones of the fan $\mathcal{T}X$. We call the underlying lattice Λ the *lineality lattice*. For example, the lineality space of a tropical hypersurface $\mathcal{T}(g)$ equals the orthogonal complement of the affine span of the Newton polytope of g , after appropriate translation to the origin. The extreme case is that of a toric variety globally parameterized by a monomial map with associated integer matrix A . Its tropicalization $\mathcal{T}X$ is a classical linear space, namely, the row span of A . $\mathcal{T}X$ coincides with its lineality space as sets with constant multiplicity *one* [10].

Since the lineality space L is contained in all cones of $\mathcal{T}X$, we can quotient the ambient space by this linear subspace, while preserving the fan structure [7]. Furthermore, we intersect this new set with the unit sphere in \mathbb{R}^{N+1}/L and consider the underlying weighted polyhedral complex. For example, if X is a surface with no non-trivial torus action, then we view $\mathcal{T}X$ as a graph in \mathbb{S}^N .

We now realize the master graph as a tropical surface in \mathbb{R}^{n+1} :

Theorem 3.2. *Fix a primitive strictly increasing sequence $(0, i_1, \dots, i_n)$ of coprime integers. Let Z be the surface in \mathbb{C}^{n+1} parameterized by $(\lambda, \omega) \mapsto (1 - \lambda, \omega^{i_1} - \lambda, \dots, \omega^{i_n} - \lambda)$. Then, the tropical surface $\mathcal{T}Z \subset \mathbb{R}^{n+1}$ coincides with the cone over the master graph as weighted polyhedral fans, with the convention that we assign the weight $m_{D_{i_1}, E_{i_1}} + m_{F_{\underline{e}}, D_{i_1}}$ to the cone over the edge $D_{i_1} E_{i_1}$ if the ending sequence $\underline{e} = \{i_1, \dots, i_n\}$ gives a node $F_{\underline{e}}$ in the master graph.*

The proof of this statement involves techniques from geometric tropicalization and resolution of plane curve singularities. Beautiful combinatorics are involved in its proof, as we show in Section 4.

Corollary 3.3. *With the notation of Theorem 3.2, the weighted graph obtained by identifying the nodes E_{i_1} and $F_{\underline{e}}$ in the master graph, and by assigning weight $i_1 + m_{F_{\underline{e}}, D_{i_1}}$ to the edge $D_{i_1} E_{i_1}$, agrees with the one-dimensional simplicial complex $\mathcal{T}Z \cap \mathbb{S}^n$.*

4. COMBINATORICS OF MONOMIAL CURVES

In this section, we compute the tropical variety of the surface Z described in Theorem 3.2. Our main tool will be the theory of *geometric tropicalization*, which we now present. The crux of this theory is to read off the tropicalization of subvarieties of tori from the combinatorics of the boundary of a suitable compactification. We describe this method for parametric surfaces.

Let f_1, \dots, f_N be Laurent polynomials in $\mathbb{C}[t_1^{\pm}, t_2^{\pm}]$ and consider the rational map $\mathbf{f}: \mathbb{T}^2 \dashrightarrow \mathbb{T}^N$, $\mathbf{f} = (f_1, \dots, f_N)$. For simplicity, we assume that the fiber of \mathbf{f} over a generic point of $Y \subset \mathbb{T}^N$ is finite. Our goal is to compute the tropicalization $\mathcal{T}Y$ of the closure of the image of the map \mathbf{f} inside the torus, without knowing its defining ideal. When the coefficients of f_1, \dots, f_N are generic with respect to their Newton polytopes, a method for constructing $\mathcal{T}Y$ from these N polytopes was given in [20, Theorem 2.1] and proved in [19, Theorem 5.1]. In the non-generic case, this question is more subtle and has been partially address in [6, 19]. For simplicity, we state the result for the case of parametric *surfaces* although the method generalizes to higher dimensional subvarieties.

Theorem 4.1 (Geometric Tropicalization [15, §2], [6, Theorems 2.5, 2.8]). *Let X be a dense open subset of \mathbb{C}^2 or \mathbb{P}^2 , and $\mathbf{f}: Y \rightarrow \mathbb{T}^N$ a generically finite Laurent polynomial map of degree δ parameterizing the surface Y . Let $X \subset \overline{X}$ be any normal and \mathbb{Q} -factorial compactification whose boundary $W = W_1 \cup \dots \cup W_k$ has combinatorial normal crossings, that is no three components intersect at a point. Let $\Delta_{\overline{X}, W}$ be the dual graph of W , i.e. the graph on $\{1, \dots, k\}$ defined by*

$$\{i, j\} \in \Delta_{\overline{X}, W} \iff W_i \cap W_j \neq \emptyset.$$

Define the integer vectors $[W_k] := (\text{val}_{W_k}(f_1), \dots, \text{val}_{W_k}(f_N)) \in \mathbb{Z}^N$ ($k = 1, \dots, k$) where $\text{val}_{W_k}(f_j)$ is the order of zero/pole of f_j along W_k . We map the abstract graph $\Delta_{\overline{X}, D}$ to a graph in

\mathbb{R}^N by sending each vertex i to $[W_i]$ and extending linearly on all edges. Define the multiplicity of the edge $([W_i], [W_j])$ to be

$$m_{([W_i], [W_j])} = \frac{1}{\delta} (W_i \cdot W_j) \text{index} \left((\mathbb{R} \otimes_{\mathbb{Z}} \mathbb{Z} \langle [W_i], [W_j] \rangle) \cap \mathbb{Z}^N : \langle [W_i], [W_j] \rangle \right),$$

where $W_i \cdot W_j$ denotes the intersection number of these divisors.

Then, the tropical surface $\mathcal{T}Y$ is the cone over this weighted graph.

Remark 4.2. With the same notation, the multiplicity of a regular point w in $\mathcal{T}Y$ equals the sum of the multiplicities of all maximal cones in $\mathcal{T}Y$ containing w .

To compute $\mathcal{T}Y$ using the previous theorems, we need a method to construct a normal \mathbb{Q} -factorial compactification $\overline{X} \supset Y$ whose boundary has *combinatorial normal crossings (CNC)*. In words, we require each number of components of the divisor W to intersect at the expected dimension. One method for producing such a compactification is taking the closure \overline{X} of X in \mathbb{P}^2 and resolving the singularities of the boundary $\overline{X} \setminus X$ to fulfill the CNC condition [6]. Along the way we record intersection numbers among the boundary components. These numbers allow us to compute tropical multiplicities, as stated in Theorem 4.1.

In what follows, we describe the resolution process of our binomial surface Z from Theorem 3.2. Roughly speaking, a full resolution gives us several extra (exceptional) divisors that yield bivalent nodes in the dual graph. If we contract these curves with negative self-intersection, we obtain a singular surface whose boundary divisor has CNC.

Recall that the surface Z was parameterized by $\mathbf{f} = (f_0, \dots, f_n): \mathbb{C}^2 \rightarrow Z$, where $f_j := \omega^{i_j} - \lambda$ ($0 \leq j \leq n$). Since geometric tropicalization involves subvarieties of tori, we restrict the domain of the function \mathbf{f} to the open set $X = \mathbb{C}^2 \setminus \bigcup_{j=0}^n (f_j = 0)$. Our task is to compactify the space X .

We now explain in full detail the compactification process. First, we naïvely compactify X inside \mathbb{P}^2 . The components of the boundary divisor of X are $D_{i_j} = (f_j^h(\omega, \lambda, u) = 0)$ and $D_\infty = (u = 0)$, where f_j^h is the homogenization of f_j with respect to the new variable u . Figure 3 illustrate this process in the case of the binomial arrangement X associated to the index set $\{0, 30, 45, 55, 78\}$ from Example 2.3. The black dots indicate the intersection of three or more of the corresponding binomial curves, whereas grey dots indicate pairwise intersections.

The boundary of X in \mathbb{P}^2 encounters three types of singularities: the origin $(0 : 0 : 1)$, the point $(0 : 1 : 0)$ at infinity, and singularities in \mathbb{T}^2 . We resolve them all by blow-ups. After contracting appropriate exceptional curves, the resolutions diagrams from Figures 4 and 5 are *precisely* the graphs on the left side of Figure 1. The nodes E_{i_j} ($1 \leq j \leq n-1$) and h_{i_j} ($2 \leq j \leq n-1$) correspond to exceptional divisors, whereas h_{i_1} refers to the strict transform of the divisor D_∞ . All intersection multiplicities involving the divisors E_{i_j} or h_{i_j} equal one. Following Theorem 4.1, we see that the computation of all multiplicities in the graph $\mathcal{T}Z$ reduces to calculating indices of suitable lattices associated to edges of $\mathcal{T}Z$.

We now describe the resolution process at the origin, whose local behavior is illustrated in the top of Figure 3. At this singular point, all n curves D_{i_1}, \dots, D_{i_n} intersect and they are tangential to each other. For any j , after a single blow-up, and after applying the change of coordinates $\lambda = w\lambda'$, we see that the strict transform of D_{i_j} is isomorphic to $D_{i_{j-1}}$ for all $1 \leq j \leq n$. This implies that we can resolve the singularity at the origin after i_{n-1} blow-ups. Moreover, we may use the previous isomorphism to compute the pull-back of each divisor D_{i_j} , one step at a time. For example, after the first blow-up π_1 , the proper transform of D_{i_j} equals $\pi_1^*(D_{i_j}) = D'_{i_j} + E_1$, where $E_1 = (w = 0)$ is the exceptional divisor and D'_{i_j} is the strict transform of D_{i_j} . After a second blow-up π_2 , we get

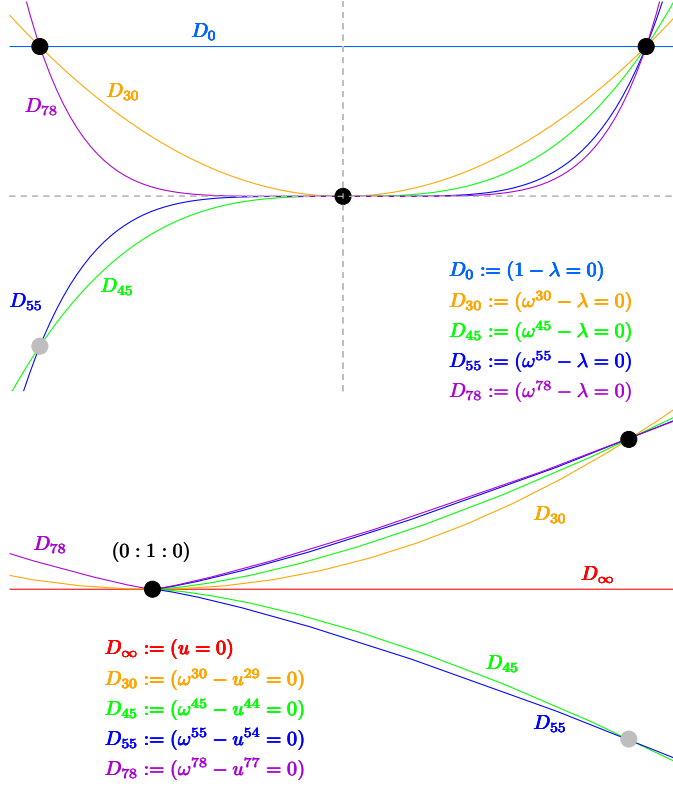


FIGURE 3. From top to bottom: $(u = 1)$ and $(\lambda = 1)$ affine charts describing the singularities of the surface \overline{X} in \mathbb{P}^2 given the set of exponents $\{0, 30, 45, 55, 78\}$.

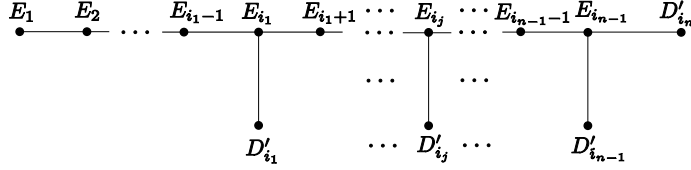


FIGURE 4. Resolution by blow-ups at the origin, where the E_{i_j} 's denote exceptional divisors and each D'_{i_j} is the strict transform of the boundary divisor D_{i_j} .

$\pi_2^*(E_1) = E'_1 + E_2$, and $\pi_2^*(D'_{i_j}) - E_2 = D''_{i_j} \simeq D_{i_j-2}$, so $(\pi_1 \circ \pi_2)^*(D_{i_j}) = D''_{i_j} + E'_1 + 2E_2$ with $D''_{i_j} \simeq D_{i_j-2}$ and $E'_1 \cdot D''_{i_j} = 0$. To simplify notation, we label all exceptional divisors by E_l and for each j we let D'_{i_j} be the strict transform of D_{i_j} under the composition π of all blow-ups. All exceptional divisors satisfy:

$$E_l \cdot E_k = \begin{cases} 1 & \text{if } |l - k| = 1, \\ 0 & \text{otherwise,} \end{cases} \quad D'_{i_j} \cdot E_l = \begin{cases} 1 & \text{if } l = i_j, \\ 0 & \text{otherwise.} \end{cases}$$

Proceeding by induction, we obtain

$$(1) \quad \pi^*(D_{i_j}) = D'_{i_j} + \sum_{l=1}^{i_j} l \cdot E_l + \sum_{l=i_j+1}^{i_{n-1}} i_j \cdot E_l \quad 1 \leq j \leq n.$$

By convention, the sum over an empty set equals 0.

Figure 4 illustrates the resolution diagram at the origin. If we eliminate the bivalent nodes E_l from Figure 4 by contracting the corresponding curves with negative self-intersection, we obtain the graph $G_{D,E}$ depicted in the left side of Figure 1, where, by abuse of notation, the strict transform of D_{i_j} is also denoted by D_{i_j} . From (1) we see that the divisorial valuation of each exceptional divisor gives the integer vector E_{i_j} described in Theorem 2.5.

At infinity, the resolution process is more delicate. The toric arrangement in the corresponding affine chart of \mathbb{P}^2 is depicted in the bottom of Figure 3. Here, the singular point $p = (0 : 1 : 0)$ corresponds to the intersection of D_∞ and all divisors D_{i_j} with $i_j \geq 2$. All prime divisors D_{i_j} , $i_j \geq 2$ have a singularity at p , so we first need to perform a blow-up at this point to smooth them out. More precisely, if π_0 denotes this blow-up we obtain

$$\pi_0^*(D_{i_j}) = D'_{i_j} + (i_j - 1)H, \quad \pi_0^*(D_\infty) = D'_\infty + H,$$

where $H = (t = 0)$ is the exceptional divisor and $D'_{i_j} = (\omega - t^{i_j-1}) \simeq D_{i_{j-1}}$, $D'_\infty = (w = 0)$ are the strict transforms of the corresponding curves.

As the reader may have discovered already, the setting after applying π_0 is very similar to the one we described for the singularity at the origin, although there are some minor local differences between them that are worth pointing out. Firstly, there is a singularity coming from the intersection of the divisors $D_{i_{s-1}}, \dots, D_{i_{n-1}}$, where s is the minimum index satisfying $i_s \geq 2$. This singular point plays the role of the origin in the chart ($u = 1$). In addition, there are two extra divisors D'_∞ and H , passing through this point. These curves had no counterpart at the chart containing the origin. Along the resolution, D'_∞ is separated from the other divisors after a single blow-up, but the strict transform of H is tangential to the strict transform of *all* divisors D'_{i_j} that meet H .

The resolution diagram at infinity is shown in Figure 5. In that picture, all exceptional divisors are denoted by h_l ($2 \leq l \leq i_n$) and we label the strict transforms of D_∞, D_{i_j} and H by D''_∞, D''_{i_j} and H' respectively. The pull-backs under the composition π of the last $i_n - 1$ blow-ups give:

$$\begin{cases} \pi^*(D'_\infty) = D''_\infty + \sum_{l=2}^{i_n} h_l, & \pi^*(H) = H' + \sum_{l=2}^{i_n} (l-1) \cdot h_l, \\ \pi^*(D'_{i_j}) = D''_{i_j} + \sum_{l=2}^{i_j} (l-1) \cdot h_l + \sum_{l=i_j+1}^{i_n} (i_j-1) \cdot h_l & (i_j \geq 2). \end{cases}$$

Composing π with the initial blow-up π_0 at the point $(0 : 1 : 0)$, we get:

$$\begin{cases} (\pi \circ \pi_0)^*(D_{i_j}) = D''_{i_j} + (i_j - 1)H' + \sum_{l=2}^{i_j} i_j(l-1) \cdot h_l + \sum_{l=i_j+1}^{i_n} (i_j-1)l \cdot h_l & (i_j \geq 2), \\ (\pi \circ \pi_0)^*(D_\infty) = H' + D''_\infty + \sum_{l=2}^{i_n} l \cdot h_l. \end{cases}$$

All intersection numbers $h_l \cdot h_{l+1}$, $h_{i_j} \cdot D''_{i_j}$, $D''_\infty \cdot h_2$ and $h_{i_n} \cdot H'$ equal one, whereas all other pairs have intersection number zero. In addition, we know that D_∞ intersects D_0 at a point, thus

$D''_\infty \cdot D_0 = 1$. Finally, the divisor D_∞ also intersects D_{i_1} at a point different from $(0 : 1 : 0)$, only if $i_1 = 1$. Thus, $D''_\infty \cdot D_1 = 1$ if $i_1 = 1$ or 0 in all other cases.

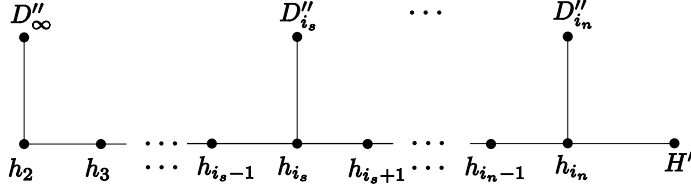


FIGURE 5. Resolution by blow-ups at infinity. Here, s is the minimum index with $i_s \geq 2$.

We now explain the transition from the resolution diagram at infinity to the graph $G_{h,D}$, depicted at the bottom-left of Figure 1. As we did when blowing up the origin, we only keep the $n - 1$ exceptional divisors h_{i_2}, \dots, h_{i_n} giving non-bivalent nodes in the resolution diagram. In addition, we contract the strict transform H' of the exceptional divisor H , since it has negative self-intersection.

The degree of the node D''_∞ in the dual graph is determined by the value of the index s . If $i_1 \geq 2$, then $s = 1$ and D''_∞ is a bivalent node adjacent to D_0 and h_{i_1} , so we remove it from the resolution diagram. On the contrary, if $i_1 = 1$, then $s = 2$ and D''_∞ has degree 3: it is adjacent to the nodes D_0 , D_1 and h_{i_2} . The node h_{i_1} in $G_{h,D}$ corresponds to the divisor D''_∞ . In both cases, and after removing all bivalent nodes and the node associated to H' , we get the graph $G_{h,D}$.

We now study multiple intersections between divisors in \mathbb{T}^2 . If (ω, λ) satisfies $f_j = \omega^{i_j} - \lambda = 0$ and $f_k = \omega^{i_k} - \lambda = 0$, then $\omega^{i_j} = \lambda = \omega^{i_k}$, so ω is a primitive r^{th} root of unity for some $r \mid (i_k - i_j)$. Equivalently, $i_j \equiv i_k \equiv u \pmod{r}$, $\omega = e^{2\pi i p/r}$ and $\lambda = \omega^u$ for some integer p coprime to r . All other curves $(f_l = 0)$ with $i_l \equiv u \pmod{r}$ also meet at (ω, λ) . We represent this crossing point by $x_{p,r,u}$ and the indices of all curves meeting at $x_{p,r,u}$ by $\underline{a}_{r,u}$, or \underline{a} for short. That is,

$$x_{p,r,u} = (e^{2\pi i p/r}, e^{2\pi i p u/r}), \quad \underline{a} = \underline{a}_{r,u} := \{i_j \mid i_j \equiv u \pmod{r}\}.$$

Furthermore, the gradients of the curves meeting at the point $x_{p,r,u}$ are pairwise independent, so the curves intersect transversally at $x_{p,r,u}$.

If three or more curves meet at a point $x_{p,r,u}$ in \mathbb{T}^2 , we blow up this point to separate the curves. After a single blow-up, we obtain a new exceptional divisor $F_{\underline{a}, x_{p,r,u}}$ which intersects the strict transform of all D_{i_j} ($i_j \in \underline{a}$) with multiplicity one. The resolution diagram is the graph $G_{F_{\underline{a}}, D}$ on the right-hand side of Figure 1, where we identify the node $F_{\underline{a}}$ with the corresponding divisor $F_{\underline{a}, x_{p,r,u}}$. From these intersection numbers, we conclude that the divisorial valuation of the exceptional divisor $F_{\underline{a}, x_{p,r,u}}$ gives $[F_{\underline{a}, x_{p,r,u}}] = \sum_{i_j \in \underline{a}} e_j$ for all intersection points $x_{p,r,u}$ coming from the same subset \underline{a} . Thus, we get a single integer vector $F_{\underline{a}} = \sum_{i_j \in \underline{a}} e_j$ in the realization of the dual graph, as desired. This explains the notation chosen for the graph $G_{F_{\underline{a}}, D}$ in Figure 1, where we accounted only for the indices of divisors intersecting at a point, rather than recording the point $x_{p,r,u}$ itself. To simplify the computation of multiplicities in the tropical surface $\mathcal{T}Z$, we also blow up crossings with $|\underline{a}| = 2$. Such blow-ups give bivalent nodes that we can easily discard in the end.

Next, we compute the divisorial valuations of all boundary components in our compactification. First, we extend the original parameterization of Z from \mathbb{T}^2 to \mathbb{P}^2 . The extended map is defined as

$$\mathbf{f}: X \subset \mathbb{P}^2 \rightarrow Z \cap \mathbb{T}^{n+1} \quad \mathbf{f}(\omega, \lambda, u) = \left(\frac{u - \lambda}{u}, \frac{\omega^{i_1} - \lambda u^{i_1-1}}{u^{i_1}}, \dots, \frac{\omega^{i_n} - \lambda u^{i_n-1}}{u^{i_n}} \right),$$

that is, $\mathbf{f}(\omega, \lambda, u) = (f_j^h(\omega, \lambda, u)/u^{\deg(f_j)})_{i=0}^n$. We compose \mathbf{f} with the resolution π to get the map $\tilde{\mathbf{f}} = \pi \circ \mathbf{f}: \tilde{X} \dashrightarrow Z \cap \mathbb{T}^{n+1}$.

We know that the functions f_0, \dots, f_n are units on X and rational functions on the closure of X in \mathbb{P}^2 : they are pullback under \mathbf{f} of the characters of \mathbb{T}^{n+1} . In particular, they have zeros and poles only along the boundary of \overline{X} . By the universal property of the blow-up, the same holds for \tilde{X} and the functions $\tilde{f}_1, \dots, \tilde{f}_n$, since they are pullback under $\tilde{\mathbf{f}}$ of the characters of \mathbb{T}^{n+1} . Therefore,

$$(\tilde{f}_0) = \pi^*(f_0) = \pi^*(D_{i_0} - D_\infty) \quad \text{and} \quad (\tilde{f}_j) = \pi^*(D_{i_j} - i_j D_\infty) \quad \text{for } j \geq 1.$$

For simplicity and to agree with the notation of the graphs in Figure 1, we denote strict transforms of all divisors with the label of the corresponding original divisors. With this convention, (\tilde{f}_j) equals

$$\begin{cases} D_{i_j} + \sum_{l=1}^{i_j} l \cdot E_l + \sum_{l=i_j+1}^{i_{n-1}} i_j \cdot E_l - D_\infty - H - \sum_{l=2}^{i_j} l \cdot h_l - \sum_{l=i_j+1}^{i_n} l \cdot h_l + \sum_{\substack{\underline{a} \ni i_j \\ x_{p,r,u}}} F_{\underline{a}, x_{p,r,u}} & \text{if } i_j < 2, \\ D_{i_j} + \sum_{l=1}^{i_j} l \cdot E_l + \sum_{l=i_j+1}^{i_{n-1}} i_j \cdot E_l - i_j \cdot D_\infty - H - \sum_{l=2}^{i_j} i_j \cdot h_l - \sum_{l=i_j+1}^{i_n} l \cdot h_l + \sum_{\substack{\underline{a} \ni i_j \\ x_{p,r,u}}} F_{\underline{a}, x_{p,r,u}} & \text{else.} \end{cases}$$

The corresponding divisorial valuations are read off from the columns of the matrix of coefficients of $(\tilde{f}_j)_{j=1}^n$ with respect to the divisors $D_{i_j}, E_{i_j}, h_{i_j}, H$ and $F_{\underline{a}, x_{p,r,u}}$. Using Theorem 4.1, we get the following nodes in the tropical variety $\mathcal{T}Z$:

$$(2) \quad \begin{cases} [D_{i_j}] = e_j, \quad [H] = -\mathbf{1}, \quad [F_{\underline{a}, x_{p,r,u}}] = \sum_{i_j \in \underline{a}} e_j, \quad [D_\infty] = -\sum_{i_j < 2} e_j - \sum_{i_j \geq 2} i_j \cdot e_j, \\ [E_l] = \sum_{l \leq i_j} l \cdot e_j + \sum_{l > i_j} i_j \cdot e_j \quad (1 \leq l \leq i_{n-1}), \\ [h_l] = -\sum_{i_j < l} l \cdot e_j - \sum_{l \leq i_j} i_j \cdot e_j \quad (2 \leq l \leq i_n). \end{cases}$$

We see that $[h_{i_n}] = i_n[H]$, so the cone over the edge $h_{i_n}H$ in the realization of the dual graph is one-dimensional. This explains why we do not see the divisor H in the graph $G_{h,D}$ from Figure 1. Likewise $i_1 \cdot [F_{i_1, \dots, i_n}] = [E_{i_1}]$ if $\gcd(i_n - i_1, \dots, i_2 - i_1) \neq 1$, so the cones over the edges $F_{i_1, \dots, i_n} D_{i_n}$ and $E_{i_1} D_{i_1}$ agree. In this case, we replace these two cones by a single cone, adding the two weights. However, these are not the only identifications we can perform to simplify our construction. The next result implies that we can eliminate the bivalent nodes E_l, h_l ($l \neq i_j$) as well as the nodes h_{i_n} and D_∞ from this graph. Roughly speaking, it says that the bivalent nodes E_{i_l} and h_{i_l} are contained in the two-dimensional cones spanned by the corresponding nodes $E_{i_j}, E_{i_{j+1}}$ and $h_{i_j}, h_{i_{j+1}}$ with $i_j < l < i_{j+1}$, and similarly for D_∞ . It also asserts that there are no overlaps between cones over the edges other than the one we already mentioned. Using these two facts we can reduce our resolution graphs to $G_{E,D}$, $G_{h,D}$, and $G_{F_{\underline{a}}, D}$, thus proving the set theoretic equality in Theorem 3.2. Recall that s is the minimum index such that $i_s \geq 2$.

Lemma 4.3. *With the notation of (2), the following have equalities hold:*

- (i) $\mathbb{R}_{\geq 0}\langle [E_l], [E_{l+1}] \rangle \cap \mathbb{R}_{\geq 0}\langle [E_{l+1}], [E_{l+2}] \rangle = \mathbb{R}_{\geq 0}\langle [E_{l+1}] \rangle$ ($i_j \leq l \leq i_{j+1} - 2$, $0 < j < n - 1$);
- (ii) $\mathbb{R}_{\geq 0}\langle [E_{i_j}], \dots, [E_{i_{j+1}}] \rangle = \mathbb{R}_{\geq 0}\langle [E_{i_j}], [E_{i_{j+1}}] \rangle$ ($1 \leq j \leq n - 2$);
- (iii) $\mathbb{R}_{\geq 0}\langle [h_l], [h_{l+1}] \rangle \cap \mathbb{R}_{\geq 0}\langle [h_{l+1}], [h_{l+2}] \rangle = \mathbb{R}_{\geq 0}\langle [h_{l+1}] \rangle$ ($2 \leq i_j \leq l \leq i_{j+1} - 2$, $0 < j < n$);
- (iv) $\mathbb{R}_{\geq 0}\langle [h_{i_j}], \dots, [h_{i_{j+1}}] \rangle = \mathbb{R}_{\geq 0}\langle [h_{i_j}], [h_{i_{j+1}}] \rangle$ ($1 \leq j \leq n - 1$);
- (v) $[h_{i_n}] \in \mathbb{R}_{\geq 0}\langle [h_{i_{n-1}}], [D_{i_n}] \rangle$;

- (vi) $\mathbb{R}_{\geq 0}\langle [E_1], \dots, [E_{i_1}] \rangle = \mathbb{R}_{\geq 0}\langle [E_{i_1}] \rangle$ and $\mathbb{R}_{\geq 0}\langle [h_2], \dots, [h_{i_s}] \rangle = \mathbb{R}_{\geq 0}\langle [h_2], [h_{i_s}] \rangle$;
- (vii) If $s = 1$, then $[D_\infty] = [h_{i_1}]$; if $s = 2$, then $\mathbb{R}_{\geq 0}\langle [D_\infty], [h_{i_1}], [h_{i_2}] \rangle = \mathbb{R}_{\geq 0}\langle [h_{i_1}], [h_{i_2}] \rangle$.

Moreover, among maximal cones over the master graph, there are no two-dimensional intersections except when $F_{\underline{e}}$ is a node in the master graph where $\underline{e} = \{i_1, \dots, i_n\}$. In this case, $i_1[F_{\underline{e}}] = [E_{i_1}]$ and $\mathbb{R}_{\geq 0}\langle [F_{\underline{e}}], [D_{i_1}] \rangle = \mathbb{R}_{\geq 0}\langle [E_{i_1}], [D_{i_1}] \rangle$.

Proof. We prove the identities involving the rays $[E_l]$ ($1 \leq l \leq i_{n-1}$) in (i) and (ii). The claims for $[h_l]$ in (iii) and (iv) can be proven analogously. Assume $i_j \leq l \leq i_{j+1} - 2$. Then $[E_{l+1}] = [E_l] + \sum_{k \geq j+1} e_k$ and $[E_{l+2}] = [E_l] + 2 \sum_{k \geq j+1} e_k$, and the first identity follows by simple linear algebra arguments.

To prove the second claim, it suffices to show that $[E_l] \in \mathbb{R}_{\geq 0}\langle [E_{i_j}], [E_{i_{j+1}}] \rangle$ if $i_j < l < i_{j+1}$. In fact, by linear algebra calculations, we obtain $[E_l] = \frac{i_{j+1}-l}{i_{j+1}-i_j} \cdot [E_{i_j}] + \frac{l-i_j}{i_{j+1}-i_j} \cdot [E_{i_{j+1}}]$. The identities in (vi) are a direct consequence of the equalities $[E_l] = l \sum_{j \geq 1} e_j = \frac{l}{i_1} [E_{i_1}]$, and $[h_l] = \frac{i_s-l}{i_s-2} [h_2] + \frac{l-2}{i_s-2} [h_{i_s}]$ for all $2 \leq l \leq i_s$.

To prove (vii) we consider all pairs of maximal cones and compute their intersection. We get either the origin or the cone over a node in the master graph. \square

Next, we compute the weights of all edges in the \mathcal{TZ} using Theorem 4.1 and the map $\tilde{\mathbf{f}}$. From the resolution \tilde{X} , we know that the intersection number of any two boundary curves is zero or one. Using Lemma 4.3, we see that there are no two-dimensional overlaps, except for the cones over the edges $D_{i_1}E_{i_1}$ and $F_{i_1, \dots, i_n}D_{i_1}$. The degree of the map $\tilde{\mathbf{f}}$ is one.

With the exception of the edge $D_{i_1}E_{i_1}$, the formula for computing weights on the edges containing D_{i_j} , h_{i_j} , E_{i_j} involves a single summand, namely the corresponding lattice index. This number is the gcd of the 2×2 -minors of a matrix whose rows are the two nodes of each edge, and it agrees with the weights assigned to the master graph.

To end, we obtain the multiplicity of the cones over the edges $F_{\underline{a}}D_{i_j}$ in \mathcal{TZ} , with $\underline{a} \neq \{i_1, \dots, i_n\}$. In this case, all summands in the formula equal one and so the multiplicity equals the number of summands. The summands are in one-to-one correspondence with the crossing points $x_{p,r,u}$, where $\underline{a} = \{i_j \mid i_j \equiv u \pmod{r}\}$ and p is coprime to r . Therefore, the number of summands is $\sum_r \varphi(r)$, where the sum is over all possible common differences r of arithmetic sequences giving the same set \underline{a} . Finally, if $\underline{e} = \{i_1, \dots, i_n\}$ gives a node $F_{\underline{e}}$ in the master graph, the divisors E_{i_1} and $F_{\underline{e}}$ map to proportional rays $[E_{i_1}]$ and $[F_{\underline{e}}]$. The multiplicities of the cones over the edges $F_{\underline{e}}D_{i_j}$ with $j \geq 2$ equal $\sum_r \varphi(r)$ for all common differences r generating the set \underline{e} . The formula to compute the weight of the edge $F_{\underline{e}}D_{i_1}$ has an extra summand: the one involving the term $E_{i_1}D_{i_1}$. Hence, $F_{\underline{e}}D_{i_1}$ has weight $m_{D_{i_1}, E_{i_1}} + m_{F_{i_1, \dots, i_n}, D_{i_1}} = i_1 + \sum_r \varphi(r)$. This concludes our proof of Theorem 3.2.

5. THE MASTER GRAPH UNDER HADAMARD PRODUCTS

In this section, we use the master graph to construct a new weighted graph: the *tropical secant graph*. This graph encodes the tropicalization of the first secant variety of a monomial projective curve C parameterized by $(1 : t^{i_1} : \dots : t^{i_n})$, where $0 = i_0 \leq i_1 \leq \dots \leq i_n$ are integers. We define the first secant variety of the curve C as

$$\text{Sec}^1(C) = \overline{\{a \cdot p + b \cdot q \mid p, q \in C, (a : b) \in \mathbb{P}^1\}} \subset \mathbb{P}^n.$$

As discussed in Section 3, tropicalizations are toric in nature. Thus, for the rest of this section, instead of looking at the projective varieties C and $\text{Sec}^1(C)$, we study the corresponding very affine varieties obtained by intersecting their affine cones in \mathbb{C}^{n+1} with the torus \mathbb{T}^{n+1} . To simplify

notation, we also denote them by C and $\text{Sec}^1(C)$. The tropicalizations of the projective varieties and their corresponding very affine varieties are the same, but we think of the projective one as living in the tropical projective torus $\mathbb{TP}^n := \mathbb{R}^{n+1}/\mathbb{R}\langle 1 \rangle$ rather than in \mathbb{R}^{n+1} , reducing its dimension by one. We parameterize the secant variety by the *secant map*

$$(3) \quad \phi: \mathbb{T}^4 \dashrightarrow \mathbb{T}^{n+1}, \quad \phi(a, b, s, t) = (as^{i_k} + bt^{i_k})_{0 \leq k \leq n}.$$

After a monomial change of coordinates $b = -\lambda a$ and $t = \omega s$, we rewrite ϕ as

$$(4) \quad \phi(a, s, \omega, \lambda) = (as^{i_k}(\omega^{i_k} - \lambda))_{0 \leq k \leq n}.$$

From this observation, it is natural to consider the Hadamard product of subvarieties of tori:

Definition 5.1. *Let $X, Y \subset \mathbb{T}^N$ be subvarieties of tori. The Hadamard product of X and Y equals*

$$X \cdot Y = \overline{\{(x_1 y_1, \dots, x_N y_N) \mid x \in X, y \in Y\}} \subset \mathbb{T}^N.$$

From the construction, we get the following characterization of our secant variety, where Z is precisely the surface Z from Theorem 3.2.

Proposition 5.2. *Let C be the monomial curve $(1 : t^{i_1} : \dots : t^{i_n})$ and let Z be the surface parameterized by $(\lambda, \omega) \mapsto (1 - \lambda, \omega^{i_1} - \lambda, \dots, \omega^{i_n} - \lambda)$. Then, the first secant variety $\text{Sec}^1(C) \subset \mathbb{T}^{n+1}$ is the Hadamard product $C \cdot Z$.*

We now explain the relationship between Hadamard products and their tropicalization:

Proposition 5.3. [7, Corollary 11] *Given C, Z as in Proposition 5.2, then as sets*

$$\mathcal{T}\text{Sec}^1(C) = \mathcal{T}C + \mathcal{T}Z,$$

where the sum on the right-hand side denotes the Minkowski sum in \mathbb{R}^{n+1} .

Since the curve C is parameterized by monomials, its tropicalization $\mathcal{T}C$ is the two-dimensional vector space spanned by the lattice vectors $\{(1, \dots, 1), (0, i_1, \dots, i_n)\}$, with constant weight one. In addition, $\mathcal{T}Z$ is a pointed polyhedral fan, and the lineality space of $\mathcal{T}\text{Sec}^1(C)$ is $\mathcal{T}C$. Thus, the associated spherical complex $(\mathcal{T}\text{Sec}^1(C)/\mathcal{T}C) \cap \mathbb{S}^{n-2}$ is a graph. It can be obtained by identifying nodes and edges in the master graph by their residue class modulo $\mathcal{T}C$. In the remainder of this section we explain this reduction process.

Before diving into the computation of $\mathcal{T}\text{Sec}^1(C)$ for any projective monomial curve C , we show that it suffices to treat the case of exponent vectors that are primitive and whose coordinates are all distinct. This simplifies the combinatorics encoded in the multiplicities as well. Here is the precise statement:

Lemma 5.4. *Via reparameterizations, we can assume that the exponent vector parameterizing the curve C is a primitive lattice vector $(0, i_1, \dots, i_n)$ with $0 = i_0 < i_1 < \dots < i_n$.*

The first claim follows by reparameterizing the curve C as $t \mapsto (1 : t^{\frac{i_1}{g}} : \dots : t^{\frac{i_n}{g}})$, where $g = \gcd(i_1, \dots, i_n)$. The second assertion is a direct consequence of the following result that shows the interplay between maps on tori and their tropicalization. Let $\alpha: \mathbb{T}^r \rightarrow \mathbb{T}^N$ be a monomial map whose exponents are encoded in a matrix $A \in \mathbb{Z}^{N \times r}$.

Theorem 5.5. [19, Theorem 3.12] *Let $V \subset \mathbb{T}^r$ be a subvariety. Then, $\mathcal{T}(\alpha(V)) = A(\mathcal{T}V)$. Moreover, if α induces a generically finite morphism of degree δ on V , the multiplicity of a regular point w of $\mathcal{T}(\alpha(V))$ is*

$$(5) \quad m_w = \frac{1}{\delta} \cdot \sum_v m_v \cdot \text{index}(\mathbb{L}_w \cap \mathbb{Z}^N : A(\mathbb{L}_v \cap \mathbb{Z}^r)),$$

where the sum is over all points $v \in \mathcal{TV}$ with $Av = w$. We also assume that the number of such v is finite and that all of them are regular points in \mathcal{TV} . In this setting, $\mathbb{L}_v, \mathbb{L}_w$ denote the linear span of neighborhoods of $v \in \mathcal{TV}$ and $w \in A(\mathcal{TV})$ respectively.

Proof of Lemma 5.4. Let $\{0, i_1, \dots, i_r\}$ be the distinct values in the exponent vector defining the curve C in increasing order. We partition the set of indices $\{0, \dots, n\}$ into $S_0 \sqcup \dots \sqcup S_r$, where each S_j consists of all indices with the same value i_j . The map

$$\alpha: \mathbb{T}^r \rightarrow \mathbb{T}^{n+1} \quad (t_1, \dots, t_r) \mapsto (\underbrace{1, \dots, 1}_{|S_0| \text{ times}}, \underbrace{t_1, \dots, t_1}_{|S_1| \text{ times}}, \dots, \underbrace{t_r, \dots, t_r}_{|S_r| \text{ times}})$$

is one-to-one and the linear map A induced by α is injective. Therefore,

$$\mathcal{T}Sec^1(\alpha(C)) = \mathcal{T}(\alpha(Sec^1(C))) = A(\mathcal{T}Sec^1(C)), \quad \mathcal{T}(\alpha(Z)) = A(\mathcal{T}Z), \quad \mathcal{T}(\alpha(C)) = A(\mathcal{T}C),$$

and any fan structure in $\mathcal{T}Sec^1(C)$ and $\mathcal{T}Z$ translates immediately to a fan structure in $\mathcal{T}Sec^1(\alpha(C))$ and $\mathcal{T}\alpha(Z)$, by the injectivity of A . From (5) we see that multiplicities match up, i.e. $m_v = m_{\alpha(v)}$ for any regular points $v, \alpha(v)$. This concludes our proof. \square

Our next goal is to explain the relationship between $\mathcal{T}Sec^1(C)$ and the *master graph* presented in Section 2. First, Proposition 5.3 expresses the tropical secant variety set-theoretically as the Minkowski sum of $\mathcal{T}C$ and $\mathcal{T}Z$. Despite what one might think at first glance, a Minkowski sum of fans does not have any canonical fan structure derived from those of its summands. Some maximal cones can be subdivided, while others can be merged into bigger cones. Nonetheless, we can still use this characterization to describe $\mathcal{T}Sec^1(C)$ not just as a set, but as a collection of four-dimensional weighted cones $\{\mathcal{T}C + \sigma\}$ where σ varies over maximal cones of $\mathcal{T}Z$ whose sum with $\mathcal{T}C$ has dimension four. This presentation allows us to compute the multiplicity of any regular point ω in $\mathcal{T}Sec^1(C)$ as the sum of weights of cones containing ω , in agreement with the spirit of Theorem 4.1 and Remark 4.2.

Each maximal cone σ in $\mathcal{T}Z$ is represented by an edge in the master graph. Thus, if we reduce the collection of four-dimensional cones encoding $\mathcal{T}Sec^1(C)$ by its lineality space $\mathcal{T}C$ and intersect it with the $(n-2)$ -sphere, we obtain a subgraph of the master graph. Intersections between cones of the collection $\mathcal{T}Sec^1(C)$ come in several flavors. If the intersection between a pair of cones is four-dimensional, we call it an *overlap*. If these cones coincide, we say the overlap is *complete*; otherwise, it is *partial*. If their intersection is three-dimensional, we call it a *crossing*. If they intersect at a common face of each, we say that the crossing is *nodal*; otherwise, it is *internal*. We wish to summarize all complete overlaps and nodal crossings in our subgraph. This data is recorded in the tropical secant graph from Definition 5.6. For a numerical example, see Figure 6. Meanwhile, partial overlaps and internal crossings are considered in Theorems 5.13, 5.14 and 6.4, when discussing fan structures. As we hinted in Theorem 3.2, a special role is played by $\underline{b} = \{0, i_1, \dots, i_{n-1}\}$ and $\underline{e} = \{i_1, \dots, i_n\}$, the “beginning” and “ending” subsets, as Remark 5.7 shows.

Definition 5.6. The tropical secant graph is a weighted subgraph of the master graph in \mathbb{R}^{n+1} , with nodes:

- (i) $D_{i_j} = e_j := (0, \dots, 0, 1, 0, \dots, 0) \quad (0 \leq j \leq n),$
- (ii) $E_{i_j} = \sum_{k < j} i_k \cdot e_k + i_j \cdot (\sum_{k \geq j} e_k) = (0, i_1, \dots, i_{j-1}, i_j, \dots, i_j) \quad (1 \leq j \leq n-1),$
- (iii) $F_{\underline{a}} = \sum_{i_j \in \underline{a}} e_j \quad \text{where } \underline{a} \subsetneq \{0, i_1, \dots, i_n\} \text{ varies among all proper subsets containing at least two elements that are obtained from an arithmetic progression.}$

The edges have positive weights:

- (i) $m_{E_{i_j}, E_{i_{j+1}}} = \gcd(i_1, \dots, i_j) \gcd_{j < t < n} (i_n - i_t) \quad (1 \leq j \leq n-2),$
- (ii) $m_{D_{i_j}, E_{i_j}} = \gcd(\gcd(i_1, \dots, i_{j-1}) \gcd_{j < l \leq n} (i_l - i_j); \gcd_{0 \leq k < j} (i_j - i_k) \gcd(i_{j+1}, \dots, i_n)) \quad (1 \leq j \leq n-1),$
- (iii) $m_{F_{\underline{a}}, D_{i_j}} = \frac{1}{2} \sum_r \varphi(r) \cdot \gcd \left(\gcd_{i_l, i_k \notin \underline{a}} (|i_l - i_k|); \gcd_{i_l, i_k \in \underline{a} \setminus \{i_j\}} (|i_l - i_k|) \right) \quad \text{where } \underline{a} = \{i_l \mid i_l \equiv i_j \pmod{r}\}, r \in \mathbb{Z} \text{ induces the subset } \underline{a} \text{ and } 2 \leq |\underline{a}| \leq n.$

(By convention, a gcd over an empty set of indices is taken to be 0.)

Remark 5.7. We explain in words the transition from the master graph to the tropical secant graph in reducing by \mathcal{TC} . First, the edges $D_{i_n} E_{i_{n-1}}$, $D_{i_n} h_{i_{n-1}}$ and $D_{i_0} h_{i_1}$ are deleted. Second, the node F_{0, i_1, \dots, i_n} and all its adjacent edges disappear. Third, the nodes h_{i_j} collapse to the corresponding nodes E_{i_j} for $1 \leq j \leq n-1$. Lastly, if $F_{\underline{a}}$ (resp. $F_{\underline{b}}$) is a node in the master graph, we identify it with E_{i_1} (resp. $E_{i_{n-1}}$) due to the equalities

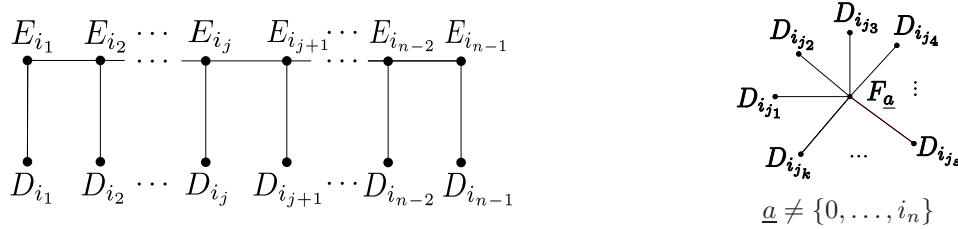
$$i_1 \cdot F_{\underline{a}} = E_{i_1}, \quad (i_n - i_{n-1}) \cdot F_{\underline{b}} = E_{i_{n-1}} + (i_n - i_{n-1}) \cdot \mathbf{1} + (-1) \cdot (0, i_1, \dots, i_n).$$

In this identification, the edges adjacent to the first node are added to those of the second. We also merge the corresponding edges $E_{i_1} D_{i_1}$ and $F_{\underline{a}} D_{i_1}$ (resp. $E_{i_{n-1}} D_{i_{n-1}}$ and $F_{\underline{b}} D_{i_{n-1}}$) in the tropical secant graph, assigning the sum of their weights to the new edge.

As in the case of the master graph, if we have a subset $\underline{a} = \{i_j, i_k\}$ coming from an arithmetic progression, then the corresponding node $F_{\underline{a}}$ is bivalent and can be removed from the tropical secant graph. We then replace the two edges $F_{\underline{a}} D_{i_j}$ and $F_{\underline{a}} D_{i_k}$ of equal weight with a single edge $D_{i_j} D_{i_k}$ of the same weight. After the above deletion of edges and collapse of nodes, some of the other nodes may also become bivalent, so we are allowed to remove them as well. However, we keep them to simplify notation.

By Theorem 1.1 the tropical secant graph characterizes the tropicalization of the first secant of any monomial curve. Here is a precise set-theoretic description of the associated graph:

Corollary 5.8. The underlying graph of $\mathcal{TSec}^1(C)$ is obtained by gluing the graphs



along all nodes D_{i_j} , and gluing together the nodes $E_{i_1} \equiv F_{i_1, \dots, i_n}$, $E_{i_{n-1}} \equiv F_{0, \dots, i_{n-1}}$.

The remainder of this section is devoted to proving Theorem 1.1, and in particular, to explaining the mysterious formulas for the weights of the tropical secant graph. We obtain these numbers using formula (5). The next propositions and lemmas characterize each one of the quantities involved in (5). Our proofs use similar techniques to the ones of [5, Lemma 4.4].

Proposition 5.9. Let $\alpha: \mathbb{T}^{2n+2} \rightarrow \mathbb{T}^{n+1}$ be the Hadamard monomial map associated to the matrix $(I_{n+1} \mid I_{n+1}) \in \mathbb{Z}^{(n+1) \times 2(n+1)}$ and C, Z as in Proposition 5.2. Then, the generic fiber of $\alpha|_{C \times Z}$ has size 2, giving $\delta = 2$ in formula (5).

Proof. Generically, by equation (4), the elements of the fiber of α at a point p are in one-to-one correspondence with pairs of points in the curve C that are collinear with p . By switching the role

of these two points in the secant map, we know that the generic fiber of $\alpha|_{C \times \mathbb{Z}}$ has size at least two. Lemma 5.10 implies that it has exactly two points. \square

Lemma 5.10. *For almost all points p in the secant variety of C , p lies on a single one secant line which, in addition, intersects the curve C at exactly two points.*

Proof. We restrict the secant map ϕ to the open torus \mathbb{T}^3 mapping $(a, s, t) \mapsto (as^{i_k} + (1-a)t^{i_k})_{0 \leq k \leq n}$. We claim that it suffices to prove the lemma for points in the image of ϕ , when $n = 4$ and the exponents are coprime and distinct

Assume the statement is true for $n = 4$ and coprime exponents. Consider all maps ϕ_j obtained by composing the map ϕ with the projections π_j onto the five coordinates $0, 1, 2, 3, j$ ($4 \leq j \leq n$). Let $d_j = \gcd(i_1, i_2, i_3, i_j)$ and reparameterize ϕ_j using the identities $x := s^{d_j}$ and $y := t^{d_j}$, that is, define $\tilde{\phi}_j: \mathbb{T}^3 \rightarrow \mathbb{C}^{n+1}$ as

$$\tilde{\phi}_j(a, x, y) := (1, ax^{\frac{i_1}{d_j}} + (1-a)y^{\frac{i_1}{d_j}}, ax^{\frac{i_2}{d_j}} + (1-a)y^{\frac{i_2}{d_j}}, ax^{\frac{i_3}{d_j}} + (1-a)y^{\frac{i_3}{d_j}}, ax^{\frac{i_j}{d_j}} + (1-a)y^{\frac{i_j}{d_j}}).$$

Since the exponents of $\tilde{\phi}_j$ are coprime and the lemma holds for $n = 4$ by assumption, we know that the fiber of $\tilde{\phi}_j$ over a point $\tilde{\phi}_j(a, x, y)$ contains only two points, namely the points (a, x, y) and $(1-a, y, x)$. Therefore, any two points (a, s, t) and (a', s', t') in the fiber of ϕ over the same point satisfies $a = a'$, $(s')^{d_j} = s^{d_j}$ and $(t')^{d_j} = t^{d_j}$ for all $4 \leq j \leq n$, up to symmetry. Since $\gcd(d_4, \dots, d_n) = 1$ we conclude $s = s'$ and $t = t'$.

We now treat the case where $n = 4$ and the exponents are coprime and pairwise distinct. To prove our result, it suffices to show that the Zariski closure of the set of points in $\text{Sec}^1(C) \setminus C$ which are intersections of two distinct secant lines of C has dimension at most two. We parameterize these points by tuples (s, t, u, v) of distinct complex numbers, corresponding to four coplanar, non-collinear points in C . It suffices to show that the set W of such tuples has dimension at most two.

The variety W is cut out by all 3×3 -minors of the 3×4 -matrix with rows $(t^{i_j} - s^{i_j})_{1 \leq j \leq 4}$, $(u^{i_j} - s^{i_j})_{1 \leq j \leq 4}$ and $(v^{i_j} - s^{i_j})_{1 \leq j \leq 4}$. Note that for all minors to vanish, it is enough to show that two of them do. We pick the ones corresponding to columns $\{1, 2, 3\}$ and $\{1, 2, 4\}$. These minors are precisely the determinants of the 4×4 generalized Vandermonde matrices

$$M_{i_1, i_2, i_3} := \begin{pmatrix} 1 & s^{i_1} & s^{i_2} & s^{i_3} \\ 1 & t^{i_1} & t^{i_2} & t^{i_3} \\ 1 & u^{i_1} & u^{i_2} & u^{i_3} \\ 1 & v^{i_1} & v^{i_2} & v^{i_3} \end{pmatrix}, \quad M_{i_1, i_2, i_4} := \begin{pmatrix} 1 & s^{i_1} & s^{i_2} & s^{i_4} \\ 1 & t^{i_1} & t^{i_2} & t^{i_4} \\ 1 & u^{i_1} & u^{i_2} & u^{i_4} \\ 1 & v^{i_1} & v^{i_2} & v^{i_4} \end{pmatrix}.$$

Because s, t, u and v are all distinct, we can divide the determinant of these two matrices by the product of pairwise differences among our four variables, that is, by the *Vandermonde determinant* $V(s, t, u, v)$. The resulting polynomials are the *Schur polynomials* S_{i_1, i_2, i_3} and $S_{i_1, i_2, i_4} \in \mathbb{Z}[s, t, u, v]$.

Let $g = \gcd(i_1, i_2, i_3)$ and $h = \gcd(i_1, i_2, i_4)$. Note that $\gcd(g, h) = 1$. By [12, Theorem 3.1] we can factorize the previous Schur polynomials over $\mathbb{Z}[s, t, u, v]$ as

$$\begin{aligned} S_{i_1, i_2, i_3} &= V(s^g, t^g, u^g, v^g) / V(s, t, u, v) \cdot T_{i_1, i_2, i_3}(s, t, u, v), \\ S_{i_1, i_2, i_4} &= V(s^h, t^h, u^h, v^h) / V(s, t, u, v) \cdot T_{i_1, i_2, i_4}(s, t, u, v), \end{aligned}$$

where T_{i_1, i_2, i_3} and T_{i_1, i_2, i_4} are either constants or irreducible over $\mathbb{C}[s, t, u, v]$. These two polynomials are homogeneous of total degree $g(i_3/g + i_2/g + i_1/g - 3)$ and $h(i_4/h + i_2/h + i_1/h - 3)$, and of degree $i_3 - 2g$ and $i_4 - 2h$ in each variable s, t, u and v . By comparing their multidegrees, we conclude that the polynomials T_{i_1, i_2, i_3} and T_{i_1, i_2, i_4} are coprime. Next, we claim that the polynomials

$V(s^g, t^g, u^g, v^g)/V(s, t, u, v)$ and $V(s^h, t^h, u^h, v^h)/V(s, t, u, v)$ are coprime. This follows from the well-known identity $(x^g - y^g) = \prod_{\zeta^g=1} (x - \zeta y)$.

From the previous two observations, we see that if S_{i_1, i_2, i_3} and S_{i_1, i_2, i_4} have a common factor, then either $V(s^h, t^h, u^h, v^h)/V(s, t, u, v)$ and T_{i_1, i_2, i_3} or the polynomials $V(s^g, t^g, u^g, v^g)/V(s, t, u, v)$ and T_{i_1, i_2, i_4} would have a common factor over $\mathbb{C}[s, t, u, v]$. Without loss of generality, assume the first pair of polynomials is not coprime. By irreducibility of T_{i_1, i_2, i_3} and the factorization of $V(s^h, t^h, u^h, v^h)$ into linear factors involving only two of the variables, this forces T_{i_1, i_2, i_3} to be linear and to involve only two variables, contradicting the degree formulas provided above. Hence, we conclude that S_{i_1, i_2, i_3} and S_{i_1, i_2, i_4} are coprime. In particular, this says that the hypersurfaces in \mathbb{C}^4 defined by S_{i_1, i_2, i_3} and S_{i_1, i_2, i_4} have distinct reduced irreducible components of dimension three. Therefore, $\dim W \leq 2$ and this ends our proof. \square

Next, we compute all cones of the form $\mathcal{TC} + \mathbb{R}_{\geq 0} \otimes \sigma$ of dimension at most three, where σ runs over edges of the master graph \mathcal{TZ} . We discard these cones from the $\mathcal{TSec}^1(C)$. In addition, we consider all possible pairs σ, σ' of such maximal cones in \mathcal{TZ} to find all pairwise intersections $(\mathcal{TC} + \mathbb{R}_{\geq 0} \otimes \sigma) \cap (\mathcal{TC} + \mathbb{R}_{\geq 0} \otimes \sigma')$ which are complete overlaps or nodal crossings. By an elementary exhaustive case by case analysis, we conclude:

Lemma 5.11. *After reducing the master graph by the linear space \mathcal{TC} , the only non-maximal cones, complete overlaps and nodal crossings are as follows:*

- (i) *The cones $\mathcal{TC} + \mathbb{R}_{\geq 0} \langle D_0, h_{i_1} \rangle$, $\mathcal{TC} + \mathbb{R}_{\geq 0} \langle D_{i_n}, E_{i_{n-1}} \rangle$, $\mathcal{TC} + \mathbb{R}_{\geq 0} \langle D_{i_n}, h_{i_{n-1}} \rangle$ and $\mathcal{TC} + \mathbb{R}_{\geq 0} \langle F_{0, i_1, \dots, i_n}, D_{i_j} \rangle$ ($0 \leq j \leq n$) are not maximal, so we disregard them.*
- (ii) *The node $F_{\{0, i_1, \dots, i_n\}} = \mathbf{1} \in \mathcal{TC}$, so we eliminate it from the graph, together with all its $n+1$ adjacent edges.*
- (iii) *For all $1 \leq j \leq n-2$, we have equalities $\mathcal{TC} + \mathbb{R}_{\geq 0} \langle E_{i_j}, D_{i_j} \rangle = \mathcal{TC} + \mathbb{R}_{\geq 0} \langle h_{i_j}, D_{i_j} \rangle$ and $\mathcal{TC} + \mathbb{R}_{\geq 0} \langle E_{i_j}, E_{i_{j+1}} \rangle = \mathcal{TC} + \mathbb{R}_{\geq 0} \langle h_{i_j}, h_{i_{j+1}} \rangle$ because $E_{i_j} \equiv h_{i_j}$ modulo \mathcal{TC} . Hence, we disregard all nodes h_{i_j} and their adjacent edges.*
- (iv) *$i_1 \cdot F_{\underline{e}} = E_{i_1}$ and $(i_n - i_{n-1}) \cdot F_{\underline{b}} \equiv E_{i_{n-1}}$ modulo \mathcal{TC} , where $\underline{e} = \{i_1, \dots, i_n\}$ and $\underline{b} = \{0, i_1, \dots, i_{n-1}\}$. Thus, the maximal cones $\mathcal{TC} + \mathbb{R}_{\geq 0} \langle F_{\underline{e}}, D_{i_1} \rangle$ and $\mathcal{TC} + \mathbb{R}_{\geq 0} \langle E_{i_1}, D_{i_1} \rangle$ coincide, as well as $\mathcal{TC} + \mathbb{R}_{\geq 0} \langle F_{\underline{b}}, D_{i_{n-1}} \rangle$ and $\mathcal{TC} + \mathbb{R}_{\geq 0} \langle E_{i_{n-1}}, D_{i_{n-1}} \rangle$.*

Proof of Theorem 1.1. Proposition 5.3 and Lemma 5.11 prove that the cone from \mathcal{TC} over the tropical secant graph coincides with the tropical variety $\mathcal{TSec}^1(C)$ as a collection of four-dimensional weighted cones. In particular, this shows that the tropical secant graph combines all nodes and edges coming from nodal crossings and complete overlaps. By formula (5), the multiplicity at a regular point ω of $\mathcal{TSec}^1(C)$ is the sum of all weights of four-dimensional cones $\mathcal{TC} + \sigma$ containing ω , where σ is a maximal two-dimensional cone of \mathcal{TZ} . Furthermore, if m_σ is the weight of σ in \mathcal{TZ} , the formula weights $\mathcal{TC} + \sigma$ by

$$\frac{1}{2} \cdot m_\sigma \cdot \text{index}((\mathbb{L}_\sigma + \mathcal{TC}) \cap \mathbb{Z}^{n+1}, (\mathbb{L}_\sigma \cap \mathbb{Z}^n) + (\mathcal{TC} \cap \mathbb{Z}^{n+1})).$$

We now prove that this number yields the weight of the corresponding edge in the tropical secant graph, after combining weights in complete overlaps following Remark 5.7. Suppose the cone σ is generated by integer vectors $\mathbf{x}, \mathbf{y} \in \mathbb{Z}^{n+1}$. Let $\mathbf{l}_1 = \mathbf{1}$ and $\mathbf{l}_2 = (0, i_1, \dots, i_n)$ be the generators of the primitive lattice Λ in $\mathcal{TC} \cap \mathbb{Z}^{n+1}$. The lattice index in the above formula is the gcd of all 4×4 -minors of the matrix $(\mathbf{x} \mid \mathbf{y} \mid \mathbf{l}_1 \mid \mathbf{l}_2)$ divided by the gcd of all 2×2 -minors of the matrix $(\mathbf{x} \mid \mathbf{y})$. These gcd's are computed as the product of the nonzero diagonal elements of the Smith normal form of each matrix.

As an example, we show how to obtain the multiplicity $m_{D_{i_j}, E_{i_j}}$ ($2 \leq j \leq n-2$). The remaining multiplicities can be computed analogously. The edge $D_{i_j} E_{i_j}$ is associated to precisely two edges in the master graph giving two four-dimensional cones in $\mathcal{T}Sec^1(C)$ that overlap completely. These two edges are $\sigma = D_{i_j} E_{i_j}$ and $\sigma' = D_{i_j} h_{i_j}$. From Definition 2.1, the multiplicity m_σ equals $\gcd(i_1, \dots, i_j)$, which is also the gcd of the 2×2 -minors of the matrix $(D_{i_j} | E_{i_j})$. Likewise, $m_{\sigma'} = \gcd(i_j, \dots, i_n)$ is the gcd of the 2×2 -minors of $(D_{i_j} | h_{i_j})$. These numbers are precisely the denominators in the formulas for computing the indices associated to σ and σ' in (2). Since $E_{i_j} \equiv h_{i_j} \pmod{\Lambda}$, we conclude

$$\begin{aligned} m_{D_{i_j}, E_{i_j}} &= \frac{1}{2} (\gcd(4 \times 4\text{-minors of } (D_{i_j} | E_{i_j} | \mathbf{l}_1 | \mathbf{l}_2)) + \gcd(4 \times 4\text{-minors of } (D_{i_j} | h_{i_j} | \mathbf{l}_1 | \mathbf{l}_2))) \\ &= \gcd(4 \times 4\text{-minors of } (D_{i_j} | E_{i_j} | \mathbf{l}_1 | \mathbf{l}_2)). \end{aligned}$$

We now compute the gcd of all 4×4 -minors of the matrix $(D_{i_j} | E_{i_j} | \mathbf{l}_1 | \mathbf{l}_2)$. For simplicity, we work with the transpose of this matrix. By elementary operations between rows that do not change the minors, we alter the second, third and fourth rows, and expand the minors along the first row, reducing our problem to computing the 3×3 -minors of the matrix

$$\begin{pmatrix} 0 & i_1 & \dots & i_{j-1} & i_j & \dots & i_j \\ 1 & 1 & \dots & 1 & 1 & \dots & 1 \\ 0 & 0 & \dots & 0 & i_{j+1} - i_j & \dots & i_n - i_j \end{pmatrix} \in \mathbb{Z}^{3 \times n},$$

where $i_0 = 0$. All non-vanishing 3×3 -minors must involve columns from the two constituent blocks. The gcd of the minors involving two columns of the left-hand side is $\gcd(i_1, \dots, i_{j-1}) \gcd_{j < l \leq n} (i_l - i_j)$, whereas the gcd of the minors involving two columns of the rightmost block equals the product $\gcd(i_1, \dots, i_j) \gcd_{j < l < n} (i_n - i_l)$. This justifies the formula for $m_{D_{i_j}, E_{i_j}}$ in Definition 5.6. \square

We now study partial overlaps and internal crossings among cones from \mathcal{TC} over edges of the tropical secant graph. An exhaustive case by case analysis shows that if $n \geq 5$, there are no partial overlaps, and that if $n \geq 6$, there are no internal crossings as well. For the case $n = 4$, Lemma 6.3 and Theorem 6.4 indicate that both partial overlaps and internal crossings are possible.

Partial overlaps and internal crossings prevent us from inferring a fan structure for $\mathcal{T}Sec^1(C)$ from the tropical secant graph. However, we may introduce new nodes at crossings, subdivide edges while preserving their weights or merge overlapping edges and their weights to create a new graph. If this surgery is performed appropriately, the new graph encodes the fan structure of our tropical variety as a subfan of the *Gröbner fan* of the homogeneous ideal defining the secant variety. This motivates the following definition:

Definition 5.12. A Gröbner tropical secant graph for a projective monomial curve C parameterized by n coprime distinct integers is a weighted graph in \mathbb{R}^{n+1} whose cone from \mathcal{TC} gives the weighted Gröbner fan structure on $\mathcal{T}Sec^1(C)$.

Unsurprisingly, the complexity of the surgery required to transform the tropical secant graph into a Gröbner tropical secant graph depends on the value of n . We present the results for $n > 4$ and postpone the discussion of the case $n = 4$ until the next section.

Theorem 5.13. The tropical secant graph of a monomial curve in \mathbb{P}^n is a Gröbner tropical secant graph for $n \geq 6$.

Proof. The proof of this result is elementary and it boils down to analyzing intersections between cones from \mathcal{TC} over pairs of edges in the tropical secant graph. If $n \geq 6$, we do not get any partial overlaps or internal crossings. \square

Theorem 5.14. *For a monomial curve in \mathbb{P}^5 , a Gröbner tropical secant graph may be constructed from the tropical secant graph by adding finitely many nodes and subdividing edges accordingly. More precisely, we must add nodes $P_{\underline{a},j,\underline{a}',k} \in (\mathcal{TC} + \langle F_{\underline{a}}, D_{i_j} \rangle) \cap (\mathcal{TC} + \langle F_{\underline{a}'}, D_{i_k} \rangle)$ where $F_{\underline{a}}, F_{\underline{a}'}$ are nodes in the master graph, and the set $\{\underline{a}, j, \underline{a}', k\}$ together with the index set $\{i_1, \dots, i_5\}$ satisfy one of the following three conditions:*

- (i) $j = 5, k = 0, i_4 + i_1 = i_2 + i_3$ and the subsets $\underline{a}, \underline{a}'$ are either $\underline{a} = \{i_3, i_4, i_5\}, \underline{a}' = \{0, i_1, i_3\}$ or $\underline{a} = \{i_2, i_4, i_5\}, \underline{a}' = \{0, i_1, i_2\}$;
- (ii) $\underline{a} = \{i_j, i_r, i_k, i_u\}, \underline{a}' = \{i_u, i_k, i_t\}, i_l \notin \underline{a} \cup \underline{a}', i_r + i_t = i_l + i_u$ and either $j > r > l > t, r > u > t$ and $u > k$, or $j < r < l < t, r < u < t$ and $u < k$;
- (iii) $\underline{a} = \{i_j, i_u, i_k, i_r\}, \underline{a}' = \{i_j, i_u, i_k, i_t\}, i_l \notin \underline{a} \cup \underline{a}'$ and $i_r + i_t = i_l + i_u$, while $j > u > k, r > l > t$ and $r > u > t$.

For each new node $P_{\underline{a},j,\underline{a}',k}$, we subdivide the edges $F_{\underline{a}}D_{i_j}$ and $F_{\underline{a}'}D_{i_k}$ of the tropical secant graph to get edges $F_{\underline{a}}P_{\underline{a},j,\underline{a}',k}, P_{\underline{a},j,\underline{a}',k}D_{i_j}$, and $F_{\underline{a}'}P_{\underline{a},j,\underline{a}',k}, P_{\underline{a},j,\underline{a}',k}D_{i_k}$, preserving the original weights.

Proof. The proof is tedious, yet elementary. As before, we consider all intersections between cones from \mathcal{TC} over edges of the tropical secant graph. While there are no partial overlaps, we have three types of internal crossings. We write down each intersection point:

- (i) Suppose $|\underline{a}| = |\underline{a}'| = 3$, say $\underline{a} = \{i_j, i_r, i_u\}, \underline{a}' = \{i_u, i_k, i_t\}$. Let $i_l \notin \underline{a} \cup \underline{a}'$. Assume the cones over the edges $F_{\underline{a}}D_{i_j}$ and $F_{\underline{a}'}D_{i_k}$ intersect and $j > k$. Then, $j = 5, r = 4, t = 1, k = 0, u = 2$ or $3, i_4 + i_1 = i_2 + i_3$ and

$$(i_r - i_l) \cdot F_{\underline{a}} + (i_j - i_r) \cdot D_{i_j} = (i_r - i_u) \cdot F_{\underline{a}'} + (i_t - i_k) \cdot D_{i_k} + (-i_l)u \cdot \mathbf{1} + (0, i_1, \dots, i_5).$$

- (ii) Suppose $|\underline{a}| = 4, |\underline{a}'| = 3$, say $\underline{a} = \{i_j, i_r, i_k, i_u\}, \underline{a}' = \{i_k, i_u, i_t\}$. Let $i_l \notin \underline{a} \cup \underline{a}'$ and assume the cones over $F_{\underline{a}}D_{i_j}$ and $F_{\underline{a}'}D_{i_k}$ intersect. Then, $i_r + i_t = i_l + i_u$ and

$$(i_r - i_l) \cdot F_{\underline{a}} + (i_j - i_r) \cdot D_{i_j} = (i_l - i_t) \cdot F_{\underline{a}'} + (i_u - i_k) \cdot D_{i_k} + (-i_l) \cdot \mathbf{1} + (0, i_1, \dots, i_5).$$

In this case, all coefficients (except for $-i_l$ and 1) have the same sign, which can be negative. If the latter occurs, we multiply the previous identity by -1 , obtaining the internal crossing of the two cones. This expression gives us up to ten extra points, determined by the inequalities $j > r > l > t, r > u > t$ and $u > k$, or $j < r < l < t, r < u < t$ and $u < k$.

- (iii) Suppose $|\underline{a}| = |\underline{a}'| = 4$, say $\underline{a} = \{i_j, i_u, i_k, i_r\}, \underline{a}' = \{i_j, i_u, i_k, i_t\}$, and assume $j > k$. Let $i_l \notin \underline{a} \cup \underline{a}'$. If the cones over $F_{\underline{a}}D_{i_j}$ and $F_{\underline{a}'}D_{i_k}$ intersect, then $i_r + i_t = i_l + i_u$ and

$$(i_r - i_l) \cdot F_{\underline{a}} + (i_j - i_u) \cdot D_{i_j} = (i_l - i_t) \cdot F_{\underline{a}'} + (i_u - i_k) \cdot D_{i_k} + (-i_l) \cdot \mathbf{1} + (0, i_1, \dots, i_5).$$

By requiring all mandatory coefficients to be positive, we obtain $j > u > k, r > l > t$ and $r > u > t$. This gives twelve possibilities for such internal crossings. \square

6. THE NEWTON POLYTOPE OF THE SECANT HYPERSURFACE IN \mathbb{P}^4

In this section, we focus our attention on monomial curves in \mathbb{P}^4 . In this situation, the first secant variety becomes a hypersurface and we wish to obtain its definition homogeneous equation from the tropical secant graph. A first step towards a complete solution would be to compute the *Newton polytope* of the defining equation f , i.e. the convex hull of all exponent vectors such that the corresponding monomial appears with a nonzero coefficient in f .

We start by summarizing the methods known to address this question. Secondly, we illustrate this technique with an example appearing in the literature [18]. We conclude the section by constructing the Gröbner tropical secant graph of any monomial curve in \mathbb{P}^4 . The latter is unnecessary for computing the associated Newton polytope, but it allows us to predict some of its rich combinatorics.

We first explain the connection between $\mathcal{T}(f)$ and $\text{NP}(f)$ for an irreducible polynomial f in $n+1$ variables defined over \mathbb{C} . For a vector $w \in \mathbb{R}^{n+1}$, the initial form $\text{in}_w(f)$ is a monomial if and only if w is in the interior of a chamber of the inner normal fan of $\text{NP}(f)$. The tropicalization of the hypersurface ($f = 0$) is the union of all the codimension one cones in the normal fan of $\text{NP}(f)$. The multiplicity of a maximal cone in $\mathcal{T}(f)$ is the lattice length of the edge of $\text{NP}(f)$ normal to that cone.

A construction of the Newton polytope $\text{NP}(f)$ from its *weighted* normal fan $\mathcal{T}(f)$ was developed in [10], and it is known as the *ray-shooting algorithm*. We describe it in Theorem 6.1 below:

Theorem 6.1. *Suppose $w \in \mathbb{R}^{n+1}$ is a generic vector so that the ray $(w + \mathbb{R}_{>0} e_i)$ intersects $\mathcal{T}(f)$ only at regular points, for all i . Let \mathcal{P}^w be the vertex of the Newton polytope \mathcal{P} of f that attains the maximum of $\{w \cdot x : x \in \mathcal{P}\}$. Then, the i^{th} coordinate of \mathcal{P}^w equals*

$$\sum_v m_v \cdot |l_i^v|,$$

where the sum is taken over all points $v \in \mathcal{T}(f) \cap (w + \mathbb{R}_{>0} e_i)$, m_v is the multiplicity of v in $\mathcal{T}(f)$, and l_i^v is the i^{th} coordinate of the primitive integral normal vector l^v to the maximal cone in $\mathcal{T}(f)$ containing v .

This theorem allows us to compute the vertices of $\text{NP}(f)$ when $\text{NP}(f)$ lies in the positive orthant and touches all coordinate hyperplanes, i.e. when f is not divisible by any non-constant monomial. Note that we do not need a fan structure on $\mathcal{T}(f)$ to use Theorem 6.1. A description of $\mathcal{T}(f)$ as a weighted set provides enough information to compute vertices of $\text{NP}(f)$ in any generic direction. Obtaining a single vertex using Theorem 6.1 gives us the multidegree of f with respect to the grading given by the intrinsic lattice Λ .

The entire polytope $\text{NP}(f)$ can be computed by iterating the ray-shooting algorithm with different objective vectors (one per chamber). A method to choose these vectors appropriately was developed in [7, Algorithm 2]: the *walking algorithm*. The core of the method is to keep track of the cones that we meet while ray-shooting from a given objective vector, and use the list of such cones to walk from chamber to chamber in the normal fan of $\text{NP}(f)$. Along the way, we pick objective vectors inside each chamber, and we repeat the shooting algorithm. We illustrate these methods with an example:

Example 6.2. The first secant variety of the monomial curve $t \mapsto (1 : t^{30} : t^{45} : t^{55} : t^{78})$ in \mathbb{P}^4 is known to be a hypersurface of degree 1820 [18, Example 3.3]. Here, we compute the tropical secant graph of the set $\{30, 45, 55, 78\}$. Using this data as input for the ray-shooting and walking algorithms, we calculate the Newton polytope of the secant threefold.

By Theorem 1.1, we encode the tropical hypersurface $\mathcal{T}\text{Sec}^1(C) \subset \mathbb{R}^5$ as a graph in \mathbb{R}^3 depicted in the left of Figure 6. The eleven nodes in the graph have coordinates $D_0 = e_0$, $D_{30} = e_1$, $D_{45} = e_2$, $D_{55} = e_3$, $D_{78} = e_4$, $E_{30} = (0, 30, 30, 30, 30)$, $E_{45} = (0, 30, 45, 45, 45)$, $F_{0,30,45,55} \equiv E_{55} = (0, 30, 45, 55, 55)$, $F_{0,30,45} = (1, 1, 1, 0, 0)$, $F_{0,30,78} = (1, 1, 0, 0, 1)$, and $F_{0,30,45,78} = (1, 1, 1, 0, 1)$. The unlabeled red nodes in the picture indicate nodes of type $F_{\underline{a}}$, where the subset \underline{a} consists of the indices of nodes D_{i_j} adjacent to it. Note that, in this example, the nodes E_{55} and $F_{0,30,45,55}$ are identified modulo the lineality space, as predicted by Definition 5.6. In particular, the edges $E_{55}D_{55}$ and $F_{0,30,45,55}D_{55}$ of the master graph coincide in the tropical secant graph and the old weights add up to $375 = 345 + 30$, as Figure 6 shows. After removing the bivalent gray node E_{30} , we have a graph with 10 nodes and 23 edges.

Finally, we apply the ray-shooting and walking algorithms to recover the Newton polytope of its defining equation. From our computation, we see that its multidegree with respect to the lattice

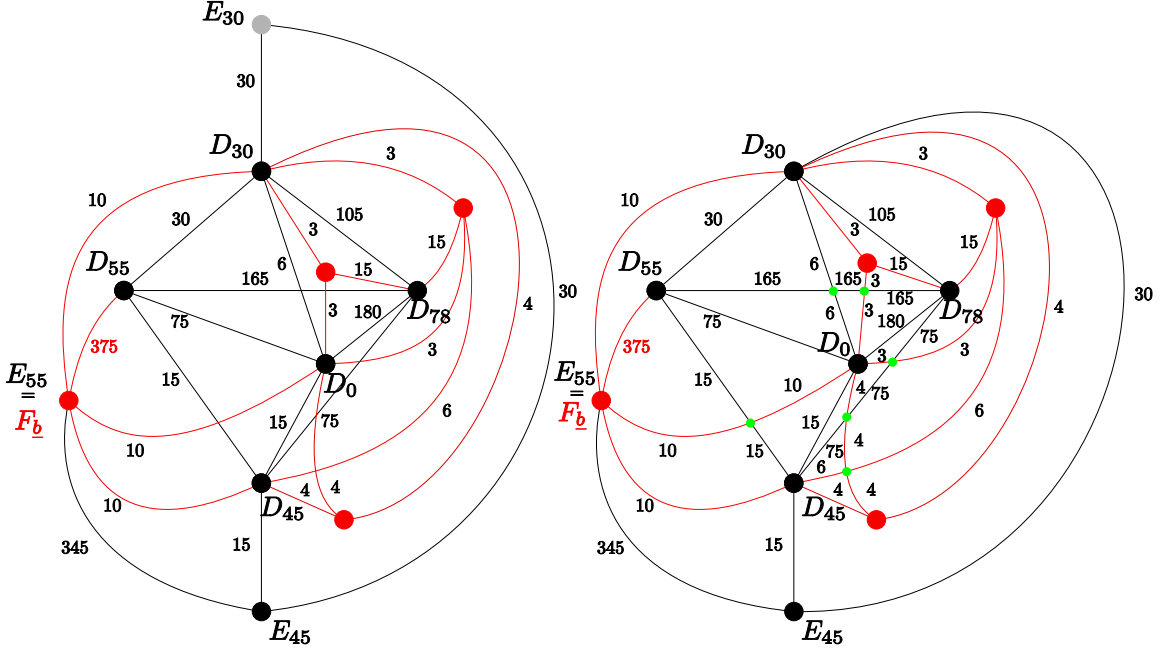


FIGURE 6. The tropical secant graph and the Gröbner tropical secant graph of the monomial curve $(1 : t^{30} : t^{45} : t^{55} : t^{78})$ in \mathbb{P}^4 .

$\Lambda = \mathbb{Z}\langle 1, (0, 30, 45, 55, 78) \rangle$ is $(1\,820, 76\,950)$, recovering the degree value from [18]. The polytope has 24 vertices and f -vector $(24, 38, 16)$. The difference between the number of facets of the polytope and the number of nodes in the tropical secant graph shows that this graph does not reflect the Gröbner fan structure of the tropical variety. In particular, we are missing six vertices which correspond to internal crossings of the graph. In the right of Figure 6, we indicate these six missing vertices with small green nodes. After adding them to the picture we obtain the Gröbner tropical secant graph of the curve C , which is a planar graph in \mathbb{S}^2 with 16 nodes and 38 edges. Each edge emanating from a new small green node corresponding to an internal crossing inherits the weight of the original edge in the tropical secant graph. The complement of this graph has 24 connected components, which matches the number of vertices of our polytope. Using **LaTTe**, we see that the polytope contains 7 566 849 lattice points, which gives an upper bound for the number of monomials in its defining equation. \diamond

We conclude the section by building the Gröbner tropical secant graph of any monomial curve in \mathbb{P}^4 . From our previous example, we already know that the tropical secant graph can be non-planar. We provide a theorem that indicates which internal crossings need to be added to make it planar. However, these are not the only possible intersections: we can have partial overlaps between edges. Luckily, there are only three types of partial overlaps. We describe them in the next lemma, which follows notation from Definition 5.6:

Lemma 6.3. *The only partial overlaps among cones in the tropical secant graph of a monomial curve in \mathbb{P}^4 are:*

- (i) $F_{i_1, i_2, i_3} D_{i_2}$ and $D_{i_2} E_{i_2}$, where $(i_4 - i_2)i_1 = (i_4 - i_3)i_2$. In this case, E_{i_2} lies in the interior of the edge $F_{i_1, i_2, i_3} D_{i_2}$, and so we replace the edge $F_{i_1, i_2, i_3} D_{i_2}$ in the tropical secant graph by the two edges $F_{i_1, i_2, i_3} E_{i_2}$ (with weight $m_{F_{i_1, i_2, i_3} D_{i_2}}$), and $D_{i_2} E_{i_2}$ (with new weight $m_{D_{i_2} E_{i_2}} + m_{F_{i_1, i_2, i_3} D_{i_2}}$).
- (ii) $F_{\underline{a}} D_{i_0}$ and $F_{\underline{a}'} D_{i_0}$, where $\underline{a} = \{0, i_l, i_t\}$ and $\underline{a}' = \{0, i_u, i_t\}$, $l > t > u$. Furthermore, if m denotes the remaining index, then $i_m + i_t = i_l + i_u$ and $l > m > u$. Hence, $F_{\underline{a}} \in F_{\underline{a}'} D_{i_0}$, and we replace the edge $F_{\underline{a}'} D_{i_0}$ by the edges $F_{\underline{a}'} F_{\underline{a}}$ (with weight $m_{F_{\underline{a}'} D_{i_0}}$), and $F_{\underline{a}} D_{i_0}$ (endowed with the new weight $m_{F_{\underline{a}} D_{i_0}} + m_{F_{\underline{a}'} D_{i_0}}$).
- (iii) $F_{\underline{a}} D_{i_j}$ and $F_{\underline{a}'} D_{i_j}$, where $\underline{a} = \{0, i_j, i_t\}$ and $\underline{a}' = \{i_j, i_t, i_u\}$. Furthermore, if m denotes the remaining index, then $i_u = i_t + i_m$. Assume $t < j$. Then, $F_{\underline{a}} \in F_{\underline{a}'} D_{i_j}$. We replace the edge $F_{\underline{a}'} D_{i_j}$ by the edges $F_{\underline{a}'} F_{\underline{a}}$ (with weight $m_{F_{\underline{a}'} D_{i_j}}$), and $F_{\underline{a}} D_{i_j}$ (changing its weight to $m_{F_{\underline{a}} D_{i_j}} + m_{F_{\underline{a}'} D_{i_j}}$). On the contrary, if $j < t$, then $F_{\underline{a}'} \in F_{\underline{a}} D_{i_j}$, and we replace the edge $F_{\underline{a}} D_{i_j}$ by the edges $F_{\underline{a}'} F_{\underline{a}}$ (with weight $m_{F_{\underline{a}} D_{i_j}}$) and $F_{\underline{a}'} D_{i_j}$ (with the new weight $m_{F_{\underline{a}} D_{i_j}} + m_{F_{\underline{a}'} D_{i_j}}$).

Proof. Let $\mathbf{l}_2 = (0, i_1, i_2, i_3, i_4)$. For any $\mu \geq 0$, each intersection point can be written as:

- (i) $\frac{i_2(i_4 - i_3)}{i_4} \cdot F_{\underline{a}} + (\frac{i_2(i_3 - i_2)}{i_4} + \mu) \cdot D_{i_2} = E_{i_2} + \mu \cdot D_{i_2} + \frac{-i_2}{i_4} \cdot \mathbf{l}_2$,
- (ii) $(i_l - i_m) \cdot F_{\underline{a}} + \mu \cdot D_{i_0} = (i_m - i_u) \cdot F_{\underline{a}'} + (i_t + \mu) \cdot D_{i_0} + (-i_m) \cdot \mathbf{1} + \mathbf{l}_2$,
- (iii) $i_m \cdot F_{\underline{a}} + (i_t + \mu) \cdot D_{i_j} = i_t \cdot F_{\underline{a}'} + (i_j + \mu) \cdot D_{i_j} + i_m \cdot \mathbf{1} - \mathbf{l}_2$. □

From the previous lemma, we get a modification of the tropical secant graph possibly with internal crossings but without partial overlaps. Finally, using this new graph, we construct the Gröbner tropical secant graph as indicated by the following theorem, which we illustrate in Example 6.5:

Theorem 6.4. *The Gröbner tropical secant graph for the monomial curve $(1 : t^{i_1} : t^{i_2} : t^{i_3} : t^{i_4})$ in \mathbb{P}^4 may be obtained by adding finitely many internal crossings to the tropical secant graph (after modifications using Lemma 6.3). These internal crossing come in two types. The first one consists of points $P_{\underline{a}, j, \underline{a}', k} \in (\mathcal{TC} + \mathbb{R}_{\geq 0} \langle F_{\underline{a}}, D_{i_j} \rangle) \cap (\mathcal{TC} + \mathbb{R}_{\geq 0} \langle F_{\underline{a}'}, D_{i_k} \rangle)$, where:*

- (i) $\underline{a} = \{i_j, i_t\}$, $\underline{a}' = \{i_j, i_t, i_l, i_k\}$, where either $j > t > s > k$ and $u > s$ or $j < t < l < k$ and $u < l$;
- (ii) $\underline{a} = \{i_j, i_t\}$, $\underline{a}' = \{i_j, i_l, i_k\}$, where either $t > u > l > k, j > l$ and $i_j + i_u \geq i_l + i_t$ or $t < u < l < k, j < s$ and $i_j + i_u \leq i_l + i_t$;
- (iii) $\underline{a} = \{i_j, i_t\}$, $\underline{a}' = \{i_t, i_l, i_k\}$, where either $u > l > k, j > t > l$ and $i_j + i_l \geq i_u + i_t$ or $u < l < k, j < t < l$ and $i_j + i_l \leq i_u + i_t$;
- (iv) $\underline{a} = \{i_t, i_j, i_u, i_k\}$, $\underline{a}' = \{i_j, i_u, i_k\}$, where either $j > u > k, t > u > k$ and $t > l$ or $j < u < k, t < u < k$ and $t < l$;
- (v) $\underline{a} = \{i_j, i_u, i_k\}$, $\underline{a}' = \{i_u, i_t, i_k\}$, where either $j > s > t, j > u > k, u > t$ and $i_j + i_t \geq i_u + i_l$ or $j < l < t, j < u < k, u < t$ and $i_j + i_t \leq i_u + i_l$;
- (vi) $\underline{a} = \{i_u, i_j, i_k\}$, $\underline{a}' = \{i_j, i_k, i_t\}$, where $u > l > t, j > t, u > k, j > k, i_l + i_j \geq i_u + i_t \geq i_l + i_k$;
- (vii) $\underline{a} = \{i_j, i_u, i_k\}$, $\underline{a}' = \{i_k, i_t\}$, where either $j > u > l > t, u > k$ and $i_u + i_t \geq i_l + i_k$ or $j < u < l < t, u < k$ and $i_u + i_t \leq i_l + i_k$;
- (viii) $\underline{a} = \{i_j, i_l, i_u, i_k\}$, $\underline{a}' = \{i_u, i_t, i_k\}$, where either $j > l > u > k$ and $u > t$ or $j < l < u < k$ and $u < t$;
- (ix) $\underline{a} = \{i_l, i_j, i_u, i_k\}$, $\underline{a}' = \{i_j, i_u, i_t, i_k\}$, where $s > u > t$ and $j > u > k$;
- (x) $\underline{a} = \{i_4, i_3, i_2\}$, $\underline{a}' = \{i_2, i_1, 0\}$, $j = 4$ and $k = 0$;
- (xi) $\underline{a} = \{i_4, i_3\}$, $\underline{a}' = \{i_1, i_0\}$, $j = 4$ and $k = 0$.

The second class satisfies $P_{j,\underline{a},k} \in (\mathcal{TC} + \mathbb{R}_{\geq 0}\langle E_{i_j}, E_{i_{j+1}} \rangle) \cap (\mathcal{TC} + \mathbb{R}_{\geq 0}\langle F_{\underline{a}}, D_{i_k} \rangle)$, where:

- (i) $\underline{a} = \{i_1, i_2, i_3\}$, $j = k = 2$ and $i_1(i_4 - i_2) \geq i_2(i_4 - i_3)$;
- (ii) $\underline{a} = \{i_1, i_2, i_4\}$, $j = k = 2$ and $i_3(i_2 - i_1) \geq i_2(i_4 - i_1)$;
- (iii) $\underline{a} = \{i_1, i_2, i_3\}$, $j = 1$, $k = 2$ and $i_4(i_2 - i_1) \geq i_2(i_3 - i_1)$;
- (iv) $\underline{a} = \{i_0, i_2, i_3\}$, $j = 1$, $k = 2$ and $i_3(i_2 - i_1) \geq i_2(i_4 - i_1)$.

Proof. The proof is very similar to the one we outlined for Theorem 5.14, so we only give the linear combination expressing each intersection point described in the statement. As usual, we let $\mathbf{l}_2 = (0, i_1, i_2, i_3, i_4) \in \Lambda \subset \mathbb{Z}^5$. The internal crossings of the first type are listed below:

- (i) For simplicity, assume $j > t > l > k$ and $u > l$ (if not, we multiply the expression by -1 to obtain the intersection point):

$$(i_t - i_l) \cdot F_{i_j, i_t} + (i_j - i_t) \cdot D_{i_j} = (i_u - i_l) \cdot F_{i_j, i_t, i_l, i_k} + (i_l - i_k) \cdot D_{i_k} - i_u \cdot \mathbf{1} + \mathbf{l}_2.$$
- (ii) Assume $i_j + i_u \geq i_l + i_t$. The intersection point is:

$$(i_t - i_u) \cdot F_{i_t, i_j} + (i_j + i_u - i_l - i_t) \cdot D_{i_j} = (i_u - i_l) \cdot F_{i_j, i_l, i_k} + (i_l - i_k) \cdot D_{i_k} - i_u \cdot \mathbf{1} + \mathbf{l}_2.$$

Note that if $i_j + i_u = i_l + i_t$, the intersection point is F_{i_j, i_t} .
- (iii) Assume $i_j + i_l \geq i_u + i_t$. The intersection point is:

$$(i_t - i_l) \cdot F_{i_t, i_j} + (i_j + i_l - i_u - i_t) \cdot D_{i_j} = (i_u - i_l) \cdot F_{i_t, i_l, i_k} + (i_l - i_k) \cdot D_{i_k} - i_u \cdot \mathbf{1} + \mathbf{l}_2.$$

Again, if $i_j + i_u = i_l + i_t$, the intersection point is F_{i_j, i_t} .
- (iv) Assume $u > k$. The intersection point is:

$$(i_t - i_l) \cdot F_{i_t, i_j, i_u, i_k} + (i_j - i_u) \cdot D_{i_j} = (i_t - i_u) \cdot F_{i_j, i_u, i_k} + (i_u - i_k) \cdot D_{i_k} - i_l \cdot \mathbf{1} + \mathbf{l}_2.$$
- (v) Assume $i_j + i_t \geq i_u + i_l$. The intersection point is:

$$(i_u - i_t) \cdot F_{i_j, i_u, i_k} + (i_j + i_t - i_u - i_l) \cdot D_{i_j} = (i_l - i_t) \cdot F_{i_u, i_t, i_k} + (i_u - i_k) \cdot D_{i_k} - i_l \cdot \mathbf{1} + \mathbf{l}_2.$$

If $i_j + i_t = i_u + i_l$, the intersection point is F_{i_j, i_u, i_k} .
- (vi) By symmetry, we can assume $j > k$. The intersection point is:

$$(i_r - i_l) \cdot F_{i_r, i_j, i_k} + (i_l + i_j - i_r - i_t) \cdot D_{i_j} = (i_l - i_t) \cdot F_{i_j, i_k, i_t} + (i_r + i_t - i_l - i_k) \cdot D_{i_k} - i_l \cdot \mathbf{1} + \mathbf{l}_2.$$

At most one of the equalities $i_l + i_j = i_r + i_t$, $i_r + i_t = i_l + i_k$ holds, and in this case, $F_{\underline{a}}$ or $F_{\underline{a}'}$ is the intersection point.
- (vii) Assume $i_r + i_t \geq i_l + i_k$. The intersection point is:

$$(i_r - i_l) \cdot F_{i_r, i_j, i_k} + (i_j - i_r) \cdot D_{i_j} = (i_l - i_t) \cdot F_{i_k, i_t} + (i_r + i_t - i_l - i_k) \cdot D_{i_k} - i_l \cdot \mathbf{1} + \mathbf{l}_2.$$

If $i_r + i_t = i_l + i_k$, the intersection point is F_{i_k, i_t} .
- (viii) Assume $u > t$. The intersection point is:

$$(i_u - i_t) \cdot F_{i_j, i_l, i_u, i_k} + (i_j - i_l) \cdot D_{i_j} = (i_l - i_u) \cdot F_{i_u, i_t, i_k} + (i_u - i_k) \cdot D_{i_k} + (i_u - i_t - i_l) \cdot \mathbf{1} + \mathbf{l}_2.$$
- (ix) The intersection point is:

$$(i_u - i_t) \cdot F_{i_j, i_l, i_u, i_k} + (i_j - i_u) \cdot D_{i_j} = (i_l - i_u) \cdot F_{i_j, i_u, i_t, i_k} + (i_u - i_k) \cdot D_{i_k} + (i_u - i_t - i_l) \cdot \mathbf{1} + \mathbf{l}_2.$$
- (x) The intersection point is:

$$(i_2 - i_1) \cdot F_{i_4, i_3, i_2} + (i_4 - i_3) \cdot D_{i_4} = (i_3 - i_2) \cdot F_{i_2, i_1, 0} + i_1 \cdot D_0 + (i_2 - i_3 - i_1) \cdot \mathbf{1} + \mathbf{l}_2.$$
- (xi) The intersection point is:

$$(i_3 - i_2) \cdot F_{i_4, i_3} + (i_4 - i_3) \cdot D_{i_4} = (i_2 - i_1) \cdot F_{i_1, i_0} + i_1 \cdot D_{i_0} - i_2 \cdot \mathbf{1} + \mathbf{l}_2.$$

We list the internal crossings of the second type:

(i) The intersection point is:

$$\frac{i_3 - i_1}{i_3 - i_2} \cdot E_{i_2} + \frac{i_1(i_4 - i_2) - i_2(i_4 - i_3)}{(i_4 - i_3)(i_3 - i_2)} \cdot E_{i_3} = i_1 \cdot F_{i_1, i_2, i_3} + (i_2 - i_1) \cdot D_{i_2} + \frac{i_1}{i_4 - i_3} \cdot \mathbf{l}_2.$$

The positivity of the coefficient of E_{i_3} gives the inequality constraint in the statement. Note that if $i_1(i_4 - i_2) = i_2(i_4 - i_3)$ then the crossing point is E_{i_2} , which is already a node in the graph, but in this case it lies in the interior of the edge $F_{i_1, i_2, i_3} D_{i_2}$.

(ii) The internal crossing is:

$$\frac{i_3}{i_3 - i_2} \cdot E_{i_2} + \frac{i_3(i_2 - i_1) - i_2(i_4 - i_1)}{(i_4 - i_3)(i_3 - i_2)} \cdot E_{i_3} = i_1 \cdot F_{i_1, i_2, i_4} + i_2 \cdot D_{i_2} - \frac{i_1}{i_4 - i_3} \cdot \mathbf{l}_2,$$

with the positivity constraint for the coefficient of E_{i_3} . If $i_3(i_2 - i_1) = i_2(i_4 - i_1)$ the crossing point is E_{i_2} and it lies in the interior of the edge $F_{i_1, i_2, i_4} D_{i_2}$.

(iii) The intersection point is:

$$\frac{i_4(i_2 - i_1) - i_2(i_3 - i_1)}{i_1(i_2 - i_1)} \cdot E_{i_1} + \frac{i_3 - i_1}{i_2 - i_1} \cdot E_{i_2} = (i_4 - i_3) \cdot F_{i_1, i_2, i_3} + (i_3 - i_2) \cdot D_{i_2} + \mathbf{l}_2,$$

with the positivity constraint for the coefficient of E_{i_1} . If $i_4(i_2 - i_1) = i_2(i_3 - i_1)$ the crossing point is E_{i_2} and it lies in the interior of the edge $F_{i_1, i_2, i_3} D_{i_2}$.

(iv) The intersection point is:

$$\frac{i_3(i_2 - i_1) - i_2(i_4 - i_1)}{i_1(i_2 - i_1)} \cdot E_{i_1} + \frac{i_4 - i_1}{i_2 - i_1} \cdot E_{i_2} = (i_4 - i_3) \cdot F_{i_0, i_2, i_3} + (i_3 - i_2) \cdot D_{i_2} - (i_4 - i_3) \cdot \mathbf{l}_1 + \mathbf{l}_2,$$

with positivity constraint for the coefficient of E_{i_1} . If $i_3(i_2 - i_1) = i_2(i_4 - i_1)$ the crossing point is E_{i_2} and it lies in the interior of the edge $F_{i_0, i_2, i_3} D_{i_2}$. \square

Example 6.5 (Example 6.2, revisited). As we saw, there are no new overlaps of edges, so Lemma 6.3 does not apply here. Using Theorem 6.4, we can explain the six new small green nodes we added to build the Gröbner tropical secant graph (Figure 6). They come from six internal crossings of the first type between the edges $F_{\underline{a}} D_{i_j}$ and $F_{\underline{a}'} D_0$, where: $\underline{a} = \{55, 78\}, j = 78, \underline{a}' = \{0, 30, 78\}$ (case (ii)); $\underline{a} = \{55, 78\}, j = 78, \underline{a}' = \{0, 30\}$ (case (xi)); $\underline{a} = \{45, 78\}, j = 78, \underline{a}' = \{0, 30, 45, 78\}$ (case (i)); $\underline{a} = \{0, 30, 45, 78\}, j = 45, \underline{a}' = \{0, 30, 45\}$ (case (iv)); $\underline{a} = \{45, 78\}, j = 78, \underline{a}' = \{0, 30, 45\}$ (case (iii)); and $\underline{a} = \{45, 55\}, j = 55, \underline{a}' = \{0, 30, 45, 55\}$ (case (i)). \diamond

7. CHOW POLYTOPES, TROPICAL SECANTS OF LINES, TORIC ARRANGEMENTS AND BEYOND

The implicitization methods discussed in the previous section can be generalized to monomial curves in higher dimensional projective spaces. In this case, one can recover the *Chow polytope* of the secant variety by a generalization of the ray-shooting algorithm, known as the *orthant-shooting* algorithm [10, Theorem 2.2]. Instead of shooting rays, we shoot orthants (i.e. cones spanned by subsets of the canonical basis of \mathbb{R}^{n+1}) of dimension equal to $n-3$ (the codimension of our variety). A formula similar to the one described in Theorem 6.1 gives us the vertex of the Chow polytope associated to a sufficiently generic input objective vector. However, it is not easy to given an analog to the walking algorithm. The difficulty comes from the fact that, a priori, there is no canonical way of walking along the complement of the tropical variety. Recently, Alex Fink has developed a method to reduce the computation of the Chow polytope to the codimension one setting, based on the orthant shooting algorithm [14]. His approach allows us to use the techniques discussed for

the secant hypersurface case [14]. Thanks to his results, existing software from [7] can be used in higher codimension examples, such as rational normal curves in \mathbb{P}^n .

Before giving a numerical example, we explain the method presented in [14] for computing Chow polytopes. We define a map, called the *Chow map* ch , which takes a tropical variety $\mathcal{T}X$ of dimension d in \mathbb{TP}^n to its *tropical Chow hypersurface*, $ch(\mathcal{T}X) = \mathcal{T}X \boxplus \mathcal{L}_{n-d-1}^{\text{refl}}$ [14, Definition 5.2]. The set $ch(\mathcal{T}X)$ is precisely the tropicalization of a hypersurface in \mathbb{P}^n whose Newton polytope equals the desired Chow polytope of X [14, Theorem 5.1].

We now describe the tropical hypersurface $ch(\mathcal{T}X)$ as the union of weighted $(n-1)$ -dimensional cones in \mathbb{TP}^n . First, we pick all weighted maximal d -dimensional cones (σ, m_σ) in $\mathcal{T}X \subset \mathbb{TP}^n$, and all $n-d-1$ cones C_J generated by subsets of $n-d-1$ vectors among $\{-e_0, -e_1, \dots, -e_n\}$, i.e. the negative of the elements in the canonical basis of \mathbb{R}^{n+1} . The subscript J indicates the indices of the vectors chosen from this basis. For simplicity, we assume that each cone σ is simplicial and that it is spanned by integer vectors $\{v_1^\sigma, \dots, v_d^\sigma\}$ in \mathbb{TP}^n . Secondly, we take the Minkowski sum of σ and C_J for every possible pair, and we check if the cone $\sigma + C_J$ in \mathbb{TP}^n has codimension 1. If so, this means that the matrix

$$A := \left(\begin{array}{c|c|c|c|c} v_1^\sigma & \dots & v_d^\sigma & -e_{j_1} & \dots & -e_{j_{n-d-1}} \end{array} \right),$$

is full dimensional, for $J = \{j_1, \dots, j_{n-d-1}\}$. We weight the new cone $\sigma + C_J$ by

$$(6) \quad m_{\sigma+C_J} := m_\sigma \cdot \gcd(\text{maximal } (n-d-1) \times (n-d-1)\text{-minors of } A).$$

If the matrix A is not of full rank, we discard the cone $\sigma + C_J$ from the list of valid combinations and we move on to the next pair. The set $ch(\mathcal{T}X)$ is the union of the valid combinations, with weights given by formula (6).

Example 7.1. The canonical example of a monomial curve in \mathbb{P}^n is the *rational normal curve* $t \mapsto (1 : t : t^2 : \dots : t^n)$. These curves and their secants have been extensively studied in the past. They are known to be determinantal varieties ([16, Proposition 9.7], [3, Proposition 2.2]) defined by the 3×3 -minors of the $j \times (n-j+2)$ *Hankel* matrix:

$$x_j := \begin{pmatrix} x_1 & x_2 & x_3 & \dots & x_{n-j+2} \\ x_2 & x_3 & \dots & \dots & \dots \\ x_3 & \dots & \dots & \dots & \dots \\ \vdots & \vdots & \vdots & \vdots & \vdots \\ x_j & x_{j+1} & \dots & x_n & x_{n+1} \end{pmatrix}.$$

The ideal generated by the 3×3 -minors of this matrix is independent of the index j [4, Corollary 2.2] and it is a set-theoretic complete intersection [21] of degree $\binom{n-1}{2}$ [4].

Using Theorem 1.1, we compute the tropical secant graph of the rational normal curve in \mathbb{P}^n . It has $n+1$ nodes $D_j = e_j$ ($0 \leq j \leq n$), $n-3$ nodes $E_j = (0, 1, 2, \dots, j, \dots, j)$ ($2 \leq j \leq n-2$) and $(\lfloor n/2 \rfloor + 1)(\lfloor n/2 \rfloor - 2)/2$ nodes $F_{\underline{a}}$, where $\underline{a} = \underline{a}_{r,u} := \{u + k \cdot r : k \in \mathbb{N}\} \cap \{0, \dots, n\}$ for some $0 \leq u < r$ and $1 < r < \lfloor n/2 \rfloor$. In addition, it has one or two nodes $F_{\underline{a}}$ where $r = \lfloor n/2 \rfloor$ and $u = 0$ (for n even), or $u = 0, 1$ (for n odd).

The graph has $2n-5$ edges labeled $E_j E_{j+1}$, ($2 \leq j \leq n-3$), $E_j D_j$ ($2 \leq j \leq n-2$), $D_1 E_2$, $E_{n-2} D_{n-1}$, with weight one. It also has edges $F_{\underline{a}_{r,u}} D_j$ ($j \in \underline{a}_{r,u}$), with weight $\varphi(r)/2$ if $r > 2$, or weight 1 if $r = 2$. In addition, it has $\lfloor n/2 \rfloor (n+3 + \lfloor n/2 \rfloor)/2$ edges $D_j D_{j+r}$ ($0 \leq j < n-r$ and $r > \lfloor n/2 \rfloor$) with weight $\varphi(r)/2$, and $\lfloor n/2 \rfloor - 2$ edges $D_j D_{j+\lfloor n/2 \rfloor}$ ($2 \leq j \leq \lfloor n/2 \rfloor$) with weight $\varphi(\lfloor n/2 \rfloor)/2$. Finally, if n is even, the edge $D_1 D_{1+n/2}$ has weight $\varphi(n/2)/2$ if $n > 2$ and weight 1 if $n = 2$.

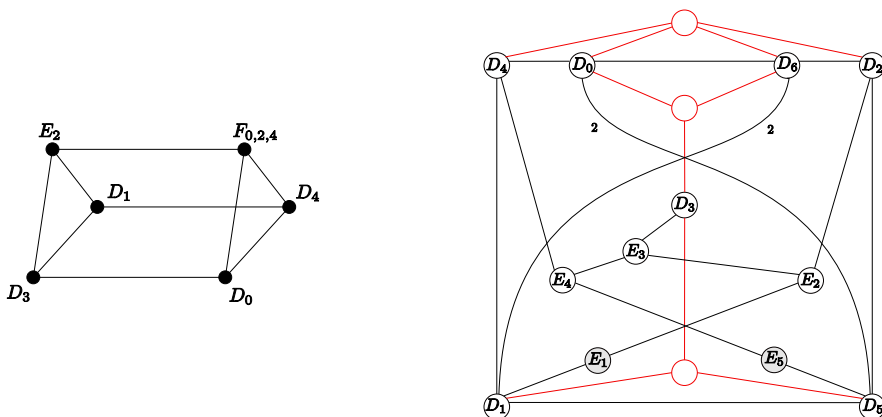


FIGURE 7. The Gröbner tropical secant graphs of the rational normal curves in \mathbb{P}^4 and \mathbb{P}^6 .

We illustrate the previous construction in the case $n = 4$. After removing the bivalent node $D_2 = e_2$, we are left with a graph with six nodes $D_0 = e_0$, $D_1 = e_1$, $D_3 = e_3$, $D_4 = e_4$, $E_2 = (0, 1, 2, 2, 2)$ and $F_{0,2,4} = (1, 0, 1, 0, 1)$ and nine edges, all with trivial weight 1. This graph is the 1-skeleton of a bipyramid (Figure 7).

Using ray-shooting and walking algorithms, we see that the equation has multidegree $(3, 6)$ with respect to the lattice $\Lambda = \mathbb{Z}\langle 1, (0, 1, 2, 3, 4) \rangle$ and its Newton polytope has vertices $(0, 0, 3, 0, 0)$, $(0, 1, 1, 1, 0)$, $(1, 0, 0, 2, 0)$, $(0, 2, 0, 0, 1)$, $(1, 0, 1, 0, 1)$, and f -vector $(5, 9, 6)$. This graph is precisely the tropical discriminant of the Veronese surface, regarded as the projectivization of the variety of all symmetric 3×3 matrices of rank at most one [10, Example 4.4]. Its defining equation is a dehomogenization of the Hankel 3×3 -determinant.

The case $n = 6$ was computed in [2, Example 20]. Its defining ideal is generated by the 3×3 -minors of the 4×4 -Hankel matrix. After changing the signs of the rays obtained by `gf an` (to agree with our *min* convention) and reducing modulo the lattice Λ , we see that our construction matches theirs for all rays except for the ones corresponding to three bivalent node E_1, E_5 and one that is absent in our graph from Figure 7 (nodes 2, 3 and 15 in the notation of [2]). We follow our convention from Example 6.2 and keep the red nodes $F_{\underline{a}}$ unlabeled. All weights in our graph equal 1, except for two edges with weight 2 (indicated in Figure 7). From this computation, we confirm that the Gröbner tropical secant graph coincides with the tropical secant graph for $n \geq 6$.

We now use the methods from [14] for computing the Chow polytope of the secant variety of the rational normal curve in \mathbb{P}^6 . In this case, the polytope has 289 vertices and f -vector $(289, 897, 981, 442, 71)$. All vertices have multidegree $(30, 90)$, which matches the formula $\deg ch(X) = \text{codim} X \cdot \deg X$ from [14, Lemma 3.4], since $30 = 3 \cdot \binom{5}{2}$.

Changing the grading to reflect the torus action by the exponent vector $(0, 1, 2, \dots, n)$ rather than the action by the all-ones vector, gives us the weighted projective space $\mathbb{P}_{(0,1,2,\dots,n)}^n$ as the ambient space, rather than the usual \mathbb{P}^n . We conjecture that this new setting results in the formula $\deg' ch(\text{Sec}^1(C)) = (n-3) \cdot \deg' \text{Sec}^1(C)$ connecting the degree of $ch(\text{Sec}^1(C))$ with respect to this exponent vector to the codimension and the degree of the secant variety of C inside this new toric variety. \diamond

We now switch gears to study the set of all tropical lines between points in the tropicalization of a monomial projective curve. We aim to highlight the differences between this set and the tropicalization of the first secant variety of the same curve. By definition, a tropical line segment between two points in the tropical curve \mathcal{TC} is the loci of all points obtained as the coordinatewise minima (i.e. tropical addition) of two fixed points in the classical plane spanned by the lattice $\Lambda = \langle \mathbf{1}, (0, i_1, \dots, i_n) \rangle$. We interpret this as the line spanned by the vector $(0, i_1, \dots, i_n)$ in \mathbb{TP}^n . The set of all tropical lines between points in \mathcal{TC} is often denoted by $S^1(\mathcal{TC})$ and it is called the *first tropical secant variety* of the line $\mathcal{TC} \subset \mathbb{TP}^n$. Since $S^1(\mathcal{TC})$ is the image of the tropicalization of the secant map ϕ from (3), we know it is contained in the tropicalization of the image of ϕ , hence $S^1(\mathcal{TC})$ is contained in $\mathcal{TSec}^1(C)$. These two tropical sets have been compared and their rich combinatorial structures has been studied by many, including Develin and Draisma [9, 11]. In particular, by [9, Corollary 2.2], we know that $S^1(\mathcal{TC})$ is a cone from \mathcal{TC} over a polytopal complex, called the *first tropical secant complex* of \mathcal{TC} . We aim to describe this complex for the case of monomial curves.

Each point in $S^1(\mathcal{TC}) \subset \mathbb{R}^{n+1}$ may be thought of as a height vector for a configuration of points $\{0, i_1, \dots, i_n\}$ on \mathbb{R} which induces a regular subdivision of the convex hull defined by these $n+1$ points. The faces of this polytopal complex correspond to regular subdivisions such that two facets cover all points. These faces are ordered by refinements of the corresponding subdivisions. Since by assumption, our exponent vector has distinct coordinates, the classical line \mathcal{TC} is *generic* in the sense of Develin, and [9, Theorem 3.1] gives a very nice characterization of this complex. It is precisely the set of lower faces of the cyclic polytope $C(2, n-1)$, defined as the convex hull of $n-1$ generic points in the parabola $\{y = x^2\} \subset \mathbb{R}^2$. It follows immediately that this complex is a chain graph with $n-1$ vertices. Figure 8 illustrates this construction for a generic classical line in \mathbb{TP}^4 .

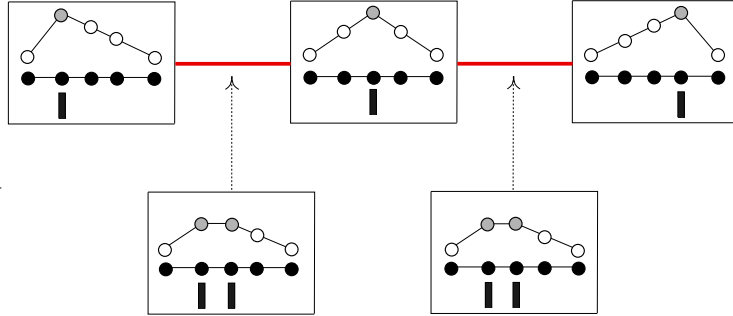


FIGURE 8. The first tropical secant complex of the line $\mathbb{R}\langle(0, i_1, i_2, i_3, i_4)\rangle$ in \mathbb{TP}^4 .

Proposition 7.2. *The first tropical secant complex of the tropicalization of the monomial curve $(1 : t^{i_1} : \dots : t^{i_n})$ (with $0 < i_1 < \dots < i_n$) is a chain graph with $n-1$ vertices $v^{(1)}, \dots, v^{(n-1)}$ embedded in \mathbb{R}^{n+1} by*

$$v^{(k)} = \sum_{j \leq k} i_j e_j + \sum_{k < j < n} \frac{i_k}{i_n - i_k} (i_n - i_j) e_j \quad k = 1, \dots, n-1.$$

Note that $v^{(k)}$ corresponds to the regular subdivision of the configuration $\{0, i_1, \dots, i_n\}$ with exactly two facets $\{0, i_1, \dots, i_k\}$ and $\{i_k, \dots, i_n\}$. It is embedded as a height vector, where the

points 0 and i_n have height zero, the point i_k has height i_k and the remaining points lie in the interior of these two facets.

Example 7.3. We describe the first secant complex of the curve $(1 : t^{30} : t^{45} : t^{55} : t^{78})$, as shown in Figure 8. It consists of three nodes $v^{(1)} = (0, 30, \frac{165}{8}, \frac{115}{8}, 0)$, $v^{(2)} = (0, 30, 45, \frac{345}{11}, 0)$ and $v^{(3)} = (0, 30, 45, 55, 0)$ and two edges $v^{(1)}v^{(2)}$ and $v^{(2)}v^{(3)}$. By taking the cone from the linear space \mathcal{TC} over this complex, we get the first tropical secant variety of the line $\mathbb{R}\langle(0, 30, 45, 55, 78)\rangle$. \diamond

We now describe $S^1(\mathcal{TC})$ as a subgraph of the tropical secant graph, and we show that the containment of $S^1(\mathcal{TC})$ in $\mathcal{TSec}^1(C)$ for a monomial curve C is strict in general.

Proposition 7.4. *In the notation of Definition 5.6, the first tropical secant complex of the tropicalization of the monomial curve $(1 : t^{i_1} : \dots : t^{i_n})$ is the chain subgraph of the tropical secant graph with nodes $E_{i_1}, \dots, E_{i_{n-1}}$.*

Proof. In the notation of Proposition 7.2, $v^{(k)}$ and E_{i_k} generate the same ray in $\mathbb{R} \otimes \Lambda$ because

$$v^{(k)} = \frac{-i_k}{i_n - i_k} \cdot (0, i_1, \dots, i_n) + \frac{i_n}{i_n - i_k} \cdot E_{i_k} \quad \text{for } k = 1, \dots, n-1.$$

The result follows immediately. \square

We finish this section by discussing briefly the relationship between our tropical secant surface graph and compactifications of toric arrangements. As we saw in Section 4, the geometric tropicalization of surfaces involves finding a suitable compactification (a *tropical compactification*) of a parametric surface inside the torus \mathbb{T}^{n+1} , or, equivalently, of the complement of $n+1$ divisors in the torus \mathbb{T}^2 . In our setting, these divisors were the $n+1$ binomial curves $\{w^{i_j} - \lambda = 0\}$ ($0 \leq j \leq n$). It is well-known that this toric arrangement can be compactified by a wonderful model in the sense of De Concini-Procesi [8]. Recently, L. Moci [17] gave an explicit compactification for toric arrangements and, at first glance, his techniques are very similar to the ones we discussed in Section 4. We hope to clarify this connection more explicit in the near future.

ACKNOWLEDGMENTS

We wish to thank Bernd Sturmfels for suggesting this project to us. We also thank Melody Chan, Alex Fink and Eric Katz for fruitful conversations. Special thanks go to Jenia Tevelev for discussions with the first author on geometric tropicalization, which led to Theorem 4.1.

REFERENCES

- [1] R. Bieri and J. Groves. The geometry of the set of characters induced by valuations. *J. Reine Angew. Math.*, 347:168–195, 1984. ISSN 0075-4102.
- [2] T. Bogart, A. N. Jensen, D. Speyer, B. Sturmfels, and R. R. Thomas. Computing tropical varieties. *J. Symbolic Comput.*, 42(1-2):54–73, 2007. ISSN 0747-7171.
- [3] M. L. Catalano-Johnson. The possible dimensions of the higher secant varieties. *Amer. J. Math.*, 118(2):355–361, 1996. ISSN 0002-9327.
- [4] A. Conca. Straightening law and powers of determinantal ideals of Hankel matrices. *Adv. Math.*, 138(2):263–292, 1998. ISSN 0001-8708.
- [5] D. Cox and J. Sidman. Secant varieties of toric varieties. *J. Pure Appl. Algebra*, 209(3):651–669, 2007. ISSN 0022-4049.
- [6] M. A. Cueto. Implicitization of surfaces via geometric tropicalization. [arXiv:1105.0509](https://arxiv.org/abs/1105.0509), 2011.

- [7] M. A. Cueto, E. A. Tobis, and J. Yu. An implicitization challenge for binary factor analysis. *J. Symbolic Comput.*, 45(12):1296–1315, 2010. ISSN 0747-7171.
- [8] C. De Concini and C. Procesi. Wonderful models of subspace arrangements. *Selecta Math. (N.S.)*, 1(3):459–494, 1995. ISSN 1022-1824.
- [9] M. Develin. Tropical secant varieties of linear spaces. *Discrete Comput. Geom.*, 35(1):117–129, 2006. ISSN 0179-5376.
- [10] A. Dickenstein, E. M. Feichtner, and B. Sturmfels. Tropical discriminants. *J. Amer. Math. Soc.*, 20(4):1111–1133 (electronic), 2007. ISSN 0894-0347.
- [11] J. Draisma. A tropical approach to secant dimensions. *J. Pure Appl. Algebra*, 212(2):349–363, 2008. ISSN 0022-4049.
- [12] R. Dvornicich and U. Zannier. Newton functions generating symmetric fields and irreducibility of Schur polynomials. *Advances in Mathematics*, 222(6):1982–2003, 2009. ISSN 0001-8708.
- [13] M. Einsiedler, M. Kapranov, and D. Lind. Non-Archimedean amoebas and tropical varieties. *J. Reine Angew. Math.*, 601:139–157, 2006. ISSN 0075-4102.
- [14] A. Fink. Tropical cycles and Chow polytopes. [arXiv:1001.4784v2](https://arxiv.org/abs/1001.4784v2), 2010.
- [15] P. Hacking, S. Keel, and J. Tevelev. Stable pair, tropical, and log canonical compactifications of moduli spaces of del Pezzo surfaces. *Invent. Math.*, 178(1):173–227, 2009. ISSN 0020-9910.
- [16] J. Harris. *Algebraic geometry, A first course*, volume 133 of *Graduate Texts in Mathematics*. Springer-Verlag, New York, 1995. ISBN 0-387-97716-3. Corrected reprint of the 1992 original.
- [17] L. Moci. Wonderful models for toric arrangements. In press, *Int. Math. Res. Not.*, [doi:10.1093/imrn/rnr016](https://doi.org/10.1093/imrn/rnr016), 2011.
- [18] K. Ranestad. The degree of the secant variety and the join of monomial curves. *Collect. Math.*, 57(1):27–41, 2006. ISSN 0010-0757.
- [19] B. Sturmfels and J. Tevelev. Elimination theory for tropical varieties. *Math. Res. Lett.*, 15(3):543–562, 2008. ISSN 1073-2780.
- [20] B. Sturmfels, J. Tevelev, and J. Yu. The Newton polytope of the implicit equation. *Mosc. Math. J.*, 7(2):327–346, 351, 2007. ISSN 1609-3321.
- [21] G. Valla. On determinantal ideals which are set-theoretic complete intersections. *Compositio Math.*, 42(1):3–11, 1980/81. ISSN 0010-437X.

MATHEMATICS DEPARTMENT, COLUMBIA UNIVERSITY, MC 4403, NEW YORK, NY, 10027, USA
E-mail address: macueto@math.columbia.edu

DEPARTMENT OF MATHEMATICS, UNIVERSITY OF CALIFORNIA, BERKELEY, CA 94720, USA
E-mail address: shaowei@math.berkeley.edu